A6

Theory of Self-Assembly of Hydrocarbon Amphiphiles into Micelles and Bilayers

BY JACOB N. ISRAELACHVILI,† D. JOHN MITCHELL AND BARRY W. NINHAM*

Department of Applied Mathematics, Institute of Advanced Studies, Research School of Physical Sciences, The Australian National University, Canberra, A.C.T. 2600, Australia

Received 7th November, 1975

A simple theory is developed that accounts for many of the observed physical properties of micelles, both globular and rod-like, and of bilayer vesicles composed of ionic or zwitterionic amphiphiles. The main point of departure from previous theories lies in the recognition and elucidation of the role of geometric constraints in self-assembly. The linking together of thermodynamics, interaction free energies and geometry results in a general framework which permits extension to more complicated self-assembly problems.

† And Department of Neurobiology, Research School of Biological Sciences, The Australian National University, Canberra.

J. Chem. Soc., Faraday Trans. II 72, pp. 1525-1568 (1976)

1. INTRODUCTION

"Despite enormous progress in understanding the genetics and biochemistry of molecular synthesis we still have only primitive ideas of how linearly synthesised molecules form the multimolecular aggregates that are cellular structures. We assume that the physical forces acting between aggregates of molecules and between individual molecules should explain many of their associative properties; but available physical methods have been inadequate for measuring or computing these forces in solids or liquids." These few succinct opening sentences from the review of V. A. Parsegian [1] embrace and define a whole grey area bridging chemistry, physics and biology which is as yet but little explored. They imply a formidable injunction. For while it is axiomatic to the physicist or chemist that structural changes in any system should be reduced to a consideration of forces or free energies which cause those changes, the burden of proof lies with the proponent. The axioms of physics do not always receive so ready an acceptance from biologists whose whole thinking in the past has been centred on the role of geometry to the almost complete exclusion of forces and entropy. The burden of proof becomes especially great if one considers the increasing sophistication of those few successful theoretical advances in our understanding of condensed matter. To be convincing, and to have any hope whatever of reducing to some semblance of order the vast complexity of those intricate multimolecular structures that are the subject of biology, any successful theories of self-assembly must have as a minimal requirement extreme simplicity—to make them accessible to the biologist who has enough concerns of his own not to be dragged into the subtleties of modern physics.

There is merit in the view that forces and entropy are important. There is merit in the view that geometry is a determining factor in self-assembly. But there have been few attempts at model self-assembly problems which embrace both views. The aim of this paper is to develop a simple theory dealing with one area of self-assembly, the spontaneous aggregation of one-component lipid suspensions, where the fusion of both notions results in a unification of a multiplicity of diverse observations.

We shall deal with ionic and zwitterionic amphiphiles. These can take on a confusing variety of different shapes and sizes: some aggregate into small spherical or globular micelles, others appear to form long cylindrical micelles, while others coalesce spontaneously into vesicular or lamellar bilayers.

The outline of the paper is as follows: In section 2 we delineate the necessary

thermodynamics which must underlie any description of self-assembly. Section 3 is concerned with the formulation of a simple model, with minimal assumptions, for the free energies of amphiphiles in both aggregated and dispersed states. In section 4 we carry out a preliminary application of the model to spherical micelles, and show that while the agreement between prediction and observation is qualitatively correct, the missing component can come only when geometric constraints are built into the model. Section 5 is devoted to a study of these geometric constraints. In section 6 thermodynamic consequences of these constraints are examined in detail, and the refined model is shown to give remarkable agreement with observation. This confidence in our model having been established, we proceed in section 7 to study its consequences for the assembly of biological phospholipids which aggregate into bilayer structures. Finally we summarise our conclusions.

2. THERMODYNAMICS OF SELF-ASSEMBLY

(a) SOME GENERAL RESULTS

To set notation and develop a framework for our later studies we briefly recapitulate the thermodynamics of micelle formation. The literature is voluminous and confusing; the most detailed statement of the problem being that of Hall and Pethica [2] based on Hill's small system thermodynamics.[3] We follow the approach of Tanford [4] in which micelles (here meaning any lipid aggregate) made up of N amphiphiles are considered to be distinct species each characterised by its own self free energy $N\mu_N^0$. N will be called the aggregation number. Assume that dilute solution theory holds. Then equilibrium thermodynamics demands that the mole fraction X_N of amphiphile incorporated into micelles of aggregation number N is given by

$$\mu_N^0+\frac{kT}{N}\ln(X_N/N) = \mu_1^0+kT\ln X_1, \tag{2.1}$$

where k is Boltzmann's constant, T is temperature, and the suffix 1 denotes isolated amphiphiles. Alternatively

$$X_N = NX_1^N \exp[N(\mu_1^0-\mu_N^0)/kT]. \tag{2.2}$$

For a prescribed total amphiphile concentration S, measured in mole fraction units, provided μ_N^0 are known functions of N and T, the X_N may be determined from eqn (2.2) together with the supplementary relation

$$S = \sum_{N=1}^{\infty} X_N. \tag{2.3}$$

Two quantities which we shall require are the mean micelle aggregation number $\bar{N}$ and the standard deviation σ of the distribution of sizes which measures polydispersity. These quantities are defined by

$$\bar{N} \equiv \sum_{N>1} NX_N / \sum_{N>1} X_N \tag{2.4}$$

$$\sigma^2 = \langle N-\bar{N}\rangle^2 = \sum_{N>1} N^2X_N / \sum_{N>1} X_N - \bar{N}^2. \tag{2.5}$$

It follows from eqn (2.2)-(2.4) that

$$\bar{N} = \frac{\partial \ln(S-X_1)}{\partial \ln X_1}. \tag{2.6}$$

This equation relates the rate of change of micelle concentration with monomer concentration to the mean micelle aggregation number. Observed aggregation

numbers $\bar{N}$ tend to be large (typically > 40) since amphiphiles can decrease their free energies significantly by forming, and only by forming, large aggregates. Therefore, an immediate consequence of eqn (2.6) is that the micelle concentrations $S-X_1$ will be rapidly varying functions of monomer concentration X_1. Define a critical micelle concentration (cmc) to be that value of X_1 for which $S-X_1^c = X_1^c$. For X_1 slightly less than the cmc X_1^c the micelle concentration will be much less than the monomer concentration, and for $X_1 > X_1^c$, the micelle concentration will be much greater than X_1. Another useful expression which follows from eqn (2.3)–(2.5) is

$$\sigma^2 = \frac{\partial \bar{N}}{\partial \ln X_1} = \bar{N}\frac{\partial \bar{N}}{\partial \ln (S-X_1)}. \tag{2.7}$$

This equation relates the standard deviation to the rate of change of mean aggregation number with respect to micelle concentration $(S-X_1)$. Clearly, a rapid change of $\bar{N}$ with concentration is evidence of a large distribution of polydispersity in micelle size (at a given concentration).

(*b*) CONSEQUENCES OF END EFFECTS

The preceding relations are standard. If $\mu_N^0-\mu_1^0$ is negative, *i.e.*, aggregates are energetically favoured, the transition from disaggregated to aggregated states comes about due to competition between entropy and energy, and little more can be said without spelling out the detailed form and magnitude of $\mu_N^0-\mu_1^0$. This will be reserved for later sections, but we anticipate here the forms which will emerge and make some general remarks. Mathematically only two possibilities exist for μ_N^0 which will allow the formation of large aggregates. We consider these in turn.

(1) μ_N^0 may have a minimum value attained for some finite value of N, say $N = M$. This is the usual case discussed in the literature.[4] Physically, such a minimum or optimal value for μ_N^0 comes about due to the competing effects, an increased hydrophobic free energy of the hydrocarbon tails for $N \lesssim M$, and increased head group interaction due to electrostatic or geometric constraints for $N \gtrsim M$. Very little can be said without a specific form of μ_N^0 and a particular example of this case will be discussed extensively in section 4. A more convenient form for eqn (2.2) is here

$$\frac{X_N}{N} = \left(\frac{X_M}{M}\exp\left[M(\mu_M^0-\mu_N^0)/kT\right]\right)^{N/M}. \tag{2.8}$$

Two points can be made. First, even if $\mu_N^0 = \mu_M^0$ for all $N > M$, as will be shown below $\bar{N}$ cannot exceed M by very much for dilute lipid solutions. In fact $\bar{N}$ will be found in section 4 to be somewhat smaller than the optimal value M. Second, if the spread of micelle size is not large, the cmc will be given to a good approximation by neglecting polydispersity and assuming $\bar{N} = M$. Whence (solving $X_1 = X_M$ for X_1^c), we have

$$\begin{aligned}\ln(\text{cmc}) &= \left(\frac{M}{M-1}\right)(\mu_M^0-\mu_1^0)/kT-\left(\frac{1}{M-1}\right)\ln M \\ &\simeq (\mu_M^0-\mu_1^0)/kT.\end{aligned} \tag{2.9}$$

This observation greatly facilitates analysis of experimental data.

(2) The other possible form for μ_N^0 is that μ_N^0 decreases with increasing N tending to a finite limit as $N \to \infty$. This form will be seen later to arise from contributions to μ_N^0 from end effects, *e.g.*, hemispherical-like ends on rod-shaped micelles, and hemicylindrical-like ends at the extremities of planar aggregates.

One functional form for μ_N^0 which will occur in connection with rod-shaped micelles is

$$\begin{aligned} \mu_N^0 &= \mu_\infty^0 + \alpha\, kT/N \qquad N \geqslant m \\ &= \infty \qquad\qquad\qquad 1 < N < m \end{aligned} \tag{2.10}$$

where α is a constant, and m is a finite number below which micelles are energetically disfavoured, *i.e.*, $\mu_N^0 \gg \mu_\infty^0$ and, therefore, for convenience μ_N^0 is set equal to infinity for $1 < N < m$. Substitution of this μ_N^0 in eqn (2.2)–(2.3) leads to

$$\frac{X_N}{N} = \mathrm{e}^{-\alpha}\, Y^N, \qquad S = X_1 + \mathrm{e}^{-\alpha} \sum_{N=m}^{\infty} NY^N, \tag{2.11}$$

where

$$Y = X_1 \exp\,(\mu_1^0 - \mu_\infty^0)/kT. \tag{2.12}$$

The summation in eqn (2.11) can be carried out to give

$$S = X_1 + \frac{mY^m\, \mathrm{e}^{-\alpha}}{1-Y}\left(1 + \frac{Y}{m(1-Y)}\right), \tag{2.13}$$

whence from eqn (2.5)

$$\bar{N} = m + \frac{Y}{1-Y}\left(1 + \frac{1}{m(1-Y)+Y}\right). \tag{2.14}$$

For small Y, in fact for $m(1-Y) \gg 1$, $\bar{N} \simeq m$ and as Y increases to 1, $\bar{N} \to \infty$. But if $m(1-Y) \ll 1$ so that $Y \approx 1$, we find

$$(S - X_1)\, \mathrm{e}^{\alpha} \simeq \frac{1}{(1-Y)^2} \gg m^2. \tag{2.15}$$

Hence $Y \approx 1$ corresponds to large and physically unreasonable micelle concentrations $(S - X_1)$ unless α is large. That is, very large micelles can only occur at reasonable concentrations (typically in the range 10^{-6}–10^{-2} mol dm^{-3}) if α is large. In this case

$$\bar{N} \simeq \frac{2}{1-Y} \simeq 2\sqrt{S\, \mathrm{e}^{\alpha}}. \tag{2.16}$$

This means that $\bar{N}$ is large and varies very rapidly with concentration S once the value of α exceeds about 25. In the other limit $m(1-Y) \gg 1$, we find

$$(S - X_1)\, \mathrm{e}^{\alpha} \simeq \frac{mY^m}{(1-Y)}. \tag{2.17}$$

This limit, therefore, corresponds to values of $(S - X_1)\, \mathrm{e}^{\alpha}$ small compared with m^2. If we take $m(1-Y) = x$ (with m large and $x \sim 1$) we have

$$\begin{aligned} \bar{N} &\simeq \frac{m(x^2+2x+2)}{x(x+1)} \\ (S - X_1)\, \mathrm{e}^{\alpha} &\simeq \frac{m^2\, \mathrm{e}^{-x}}{x} \end{aligned} \tag{2.18}$$

so that if x is chosen to make $(S - X_1)\, \mathrm{e}^{\alpha} \simeq 1$, we have $\bar{N} \simeq m$. Therefore, with the form of μ_N^0 given by eqn (2.10), when α is small only small micelles ($\bar{N} \simeq m$) can occur at reasonable micelle concentrations $(S - X_1) \ll 1$. These micelles will be narrowly dispersed. When α is large, micelles will be large and broadly dispersed.

Another form which will be of interest in connection with the formation of bilayers is

$$\mu_N^0 = \mu_\infty^0 + \alpha\frac{kT}{N^{\frac{1}{2}}} \qquad N \geqslant m$$
$$= \infty \qquad 1 < N < m \tag{2.19}$$

which leads to the expression for the concentration

$$S = X_1 + \sum_{N=m}^{\infty} NY^N \exp(-\alpha N^{\frac{1}{2}}), \tag{2.20}$$

where Y is given by eqn (2.12). This series has the property of converging on its circle of convergence ($|Y| = 1$), which leads to an interesting consequence. For a sufficiently large α, it will converge to a value of $S \ll 1$ for $Y = 1$. Once this concentration is exceeded the amphiphiles will assemble spontaneously into infinite bilayers. ($Y = 1$ or $\mu_1^0 + kT \ln X_1 = \mu_\infty^0$ is equivalent to the condition that the chemical potential of amphiphiles in solution equals that of amphiphiles incorporated into infinite bilayers.) It is possible that the system will have a cmc before it reaches this phase transition.

Consider as yet another possible example

$$\mu_N^0 = \mu_\infty^0 + \alpha kT/N^2; \qquad N \geqslant m \tag{2.21}$$

which we shall use to illustrate the case when $\mu_N^0 - \mu_\infty^0$ vanishes faster than $1/N$. We find now

$$S - X_1 = \sum_{N=m}^{\infty} NY^N e^{-\alpha/N}. \tag{2.22}$$

Since the result does not depend significantly on the lower limit of the sum when $N > m$ we shall replace m by 1 for convenience.

Consider the sum

$$\sum = \sum_{1}^{\infty} Y^N e^{-\alpha/N} = \tfrac{1}{2}\sum_{-\infty}^{\infty} e^{-\beta|N|-\alpha/|N|}, \tag{2.23}$$

where $\beta = -\ln Y$. Applying the Poisson summation formula [5] to this, we find

$$\sum = \tfrac{1}{2}\sum_{N=-\infty}^{\infty}\int_{-\infty}^{\infty} e^{2\pi i Nx} e^{-\beta|x|-\alpha/|x|}\,dx$$
$$= \int_0^\infty e^{-\beta x-\alpha/x}\,dx + 2\sum_1^\infty \int_0^\infty \cos(2\pi Nx)\, e^{-\beta x-\alpha/x}\,dx. \tag{2.24}$$

By the substitution $x = y\sqrt{\alpha/\beta}$, this equation may be written

$$\sum = \left(\frac{\alpha}{\beta}\right)^{\frac{1}{2}}\int_0^\infty \exp\{-(\alpha\beta)^{\frac{1}{2}}(y+1/y)\}\,dy +$$
$$2\sum_1^\infty\left(\frac{\alpha}{\beta}\right)^{\frac{1}{2}}\int_0^\infty \cos\left[2\pi N\left(\frac{\alpha}{\beta}\right)^{\frac{1}{2}} y\right]\exp\{-(\alpha\beta)^{\frac{1}{2}}(y+1/y)\}\,dy. \tag{2.25}$$

Consequently if $\beta = -\ln Y$ is small and α large, which is the limit of most interest to us, the period of the cosine in the integrand of eqn (2.25) is much smaller than the width of the exponential term (the precise condition for this is $\alpha^{\frac{1}{2}}/\beta^{\frac{3}{2}} \gg 1$) and consequently the sum of eqn (2.25) may be neglected leaving

$$\sum \approx \left(\frac{\alpha}{\beta}\right)^{\frac{1}{2}}\int_0^\infty \exp\{-(\alpha\beta)^{\frac{1}{2}}(y+1/y)\}\,dy. \tag{2.26}$$

Let us further restrict ourselves to the case $(\alpha\beta)^{\frac{1}{2}} \gg 1$. The integral may then be evaluated by the method of steepest descents,[6] yielding

$$\sum \approx \frac{\pi^{\frac{1}{2}}\alpha^{\frac{1}{2}}}{\beta^{\frac{1}{2}}} e^{-2\sqrt{\alpha\beta}}. \tag{2.27}$$

Therefore

$$S-X_1 = -\frac{\partial}{\partial\beta}\sum \simeq \frac{\pi^{\frac{1}{2}}\alpha^{\frac{1}{2}}}{\beta^{\frac{1}{2}}} e^{-2\sqrt{\alpha\beta}} \tag{2.28}$$

and

$$\bar{N} = -\frac{\partial}{\partial\beta}\ln(S-X_1) \simeq \sqrt{\alpha/\beta}. \tag{2.29}$$

This allows us to rewrite (2.28) as

$$S-X_1 = \frac{\pi^{\frac{1}{2}}}{\alpha^{\frac{1}{2}}}\bar{N}^{\frac{1}{2}} e^{-2\alpha/\bar{N}}, \tag{2.30}$$

giving us an implicit expression for $\bar{N}$ as a function of $S-X_1$. We have made the approximations $(\alpha\beta)^{\frac{1}{2}} \simeq \alpha/\bar{N} \gg 1$ and $\alpha^{\frac{1}{2}}/\beta^{\frac{1}{2}} = \bar{N}^{\frac{1}{2}}/\alpha \gg 1$, *i.e.*, $\bar{N} \ll \alpha \ll \bar{N}^{\frac{1}{2}}$. One sees immediately from eqn (2.30) that under these conditions a large change in lipid concentration $S-X_1$ is required to produce a significant change in $\bar{N}$, *i.e.*, $\bar{N}$ is a slowly varying function of $S-X_1$. In order that N may be a rapidly varying function of $S-X_1$, it would be necessary that $\alpha \sim \bar{N}$, whereupon $S-X_1$ would be unphysically large. We conclude, therefore, that the form (2.21) would lead to lipid aggregates with little polydispersity. More generally, it can be shown that for a system with a chemical potential of the form $\mu_N^0 = \mu_\infty^0 + \alpha kT/N^P$, a phase transition to macroscopic aggregates will occur only if $P < 1$. For $P > 1$, the system will be narrowly dispersed about a finite aggregation number. When $P = 1$, the system will be broadly dispersed with a large aggregation number which is very sensitive to total amphiphile concentration.

3. FORMULATION OF A MODEL FOR THE FREE ENERGIES

No further progress can be made without some explicit model which gives the free energies μ_N^0, μ_1^0 per amphiphile in both the aggregated and dispersed states. First consider the aggregated state. Contributions to the free energy μ_N^0 fall into two classes, bulk and surface terms. It is well established that for most amphiphiles their hydrocarbon interiors in micelles and bilayers are in a liquid-like state above 0°C.[4, 7-11] Hence the bulk free energy per amphiphile, g, will be a function only of temperature T and the number of carbon atoms n. Surface contributions are of two kinds: (1) those arising from the attractive hydrophobic or surface tension forces, and (2) from opposing repulsive forces, in main of electrostatic origin. Since the hydrocarbon interior exists in a liquid-like state, we expect that the attractive force contribution can be well represented by an interfacial free energy per unit area of aggregate γ, where γ is close to 50 erg cm^{-2} characteristic of the liquid hydrocarbon–water interface. This value has been shown to be essentially the surface tension of water minus the dispersion energy contributions at the water–hydrocarbon interface.[12, 13] As the surface tension of water varies by < 1 % over the range 0–0.5 mol dm^{-3} NaCl,[14] we can expect the interfacial tension to be likewise insensitive to ionic strength. The surface area a per amphiphile is measured at the hydrocarbon–water interface, and the choice of this interface is a contentious issue. Herman [15] and Tanford *et al.*[4, 16] choose this interface at a distance equal to the radius of one

water molecule beyond the van der Waals boundary of the outermost methylene groups. (Since dispersion contributions to γ are negligible, this is equivalent to choosing the Gibbs dividing surface as the interface.) There appears to be no substantial reason for this choice. Indeed, thermodynamic arguments,[17] together with an analysis of some solubility data,[18] show that for various molecules the interface should be taken at, or even inside, the van der Waals boundary. We take the van der Waals boundary to define the interface. It will be seen subsequently that this choice goes some way towards removing a puzzling anomaly in our understanding of hydrophobic interactions. We remark on one further problem in defining surface tension contributions: The question as to whether we should take γa or $\gamma(a-a')$, where a' is the area per amphiphile covered by the head group and therefore not in direct contact with water. Since $\gamma a'$ is constant, it can be absorbed into the bulk term g, to which it makes a small contribution.

The repulsive surface terms are much more difficult to handle. The shape, size, and orientation of charged head groups, surface charge density, specific ionic adsorption, unknown dielectric constant of the surface region, certain occurrence of Stern layers and associated discreteness of charge effects all conspire to inhibit any rigorous analysis. For example, in recent work on ionic micelles, Stigter [11] showed that use of a Chapman–Gouy model for the double layer based on the non-linear Poisson–Boltzmann equation gives an outward electrostatic pressure which varies by only 20 % over an electrolyte concentration of 0–0.4 mol dm^{-3} NaCl. On the other hand, the cruder Debye–Hückel approximation taken with an arbitrary factor of the order of $\frac{1}{2}$ gives a reasonable description of the critical micelle concentration and other properties of ionic lipid micelles.[4, 19, 20] As regards the Stern layer, Stigter[11, 21] has carried out an analysis for a variety of ionic micelles and concludes that the counterions are effectively in a layer of thickness 4–5 Å. Despite the apparent intractability of the problem, the various approaches suggest that all of these complications can be subsumed by simple phenomenological forms. Various authors since Debye [22] have attempted such an analysis.[11, 19-26] Thus, a repulsive energy contribution which varies as a constant/a has been shown by Tanford [19] to give a realistic description of micelle size and cmc. A repulsive energy of this form would arise from a double layer of charge as in a capacitor, with charge e/a per unit area, separation D of the capacitor planes, and dielectric constant ε. The magnitude of the constant is then $2\pi e^2 D/\varepsilon$. We adopt this form.

We stress that this choice for the repulsive energy is not critical. All the subsequent analysis can be carried out with other repulsive forms, *e.g.*, constant/a^2. The advantage of the capacitance model is that it gives about the simplest expression for the energy with any semblance of physical reality which is amenable to exact analysis. Such an assumption clearly disguises a multitude of sins, and can only be justified *a posteriori*.

One further advantage of this form is that for zwitterionic amphiphiles where the head groups are normal to the surface (*e.g.*, as is believed to be the case for lecithin [27, 28]), the value of D can be readily identified with zwitterionic charge group separation. The expression we have chosen is to be expected here (see Appendix A). Additional support for the universal phenomenological form constant/a is furnished by the observation [29] that both ionic and zwitterionic amphiphiles have very similar micellar properties. If these assumptions are granted, the free energy μ_N^0 per amphiphile in the aggregate is

$$\mu_N^0 = \gamma a + \frac{2\pi e^2 D}{\varepsilon a} + g. \qquad (3.1)$$

(a) CURVATURE CORRECTIONS

The form eqn (3.1) is to hold strictly for planar surfaces. We have already alluded to curvature corrections to the effective surface tension contribution. If the micellar surface is spherical, the effective surface tension γ for both a drop and a hole in the liquid is less than that for a planar interface by a factor $(1-\delta/R)$, where δ is of the order of one or two molecular radii and R is the position of the Gibbs dividing surface.[17, 18] Corresponding corrections to the electrostatic contributions are expected to be of much more importance, and can be handled within the framework of a capacitance description. Thus for a spherical capacitance the energy per unit area is from electrostatics

$$E_s = \frac{2\pi e^2 D}{\varepsilon a(1+D/R)}. \tag{3.2}$$

Except for two instances in the subsequent development, curvature corrections can be ignored.

(b) MONOMER FREE ENERGY

The monomer free energy μ_1^0 comprises two main contributions, a hydrophobic term g' due to the self-energy of the hydrocarbon chain in water, and an electrostatic self-energy associated with the (charged) head group. The term g' is undefined by itself, but the important quantity $g'-g$ has a meaning as the usual hydrophobic energy [4] required to take a hydrocarbon chain from water to bulk hydrocarbon. For this quantity we use the measured value so that a precise model for this contribution is unnecessary. Characteristically [4] $g'-g \simeq 825$ cal mol^{-1} (CH_2 group)$^{-1}$ and 2100 cal mol^{-1} (CH_3 group)$^{-1}$. (We note in passing that in analysing the measured hydrophobic free energy changes for n-alkanes, various authors [15, 16] assign a value to the hydrophobic interfacial energy of $\gamma_h = 20$–33 cal mol^{-1} Å^{-2}, equivalent to 14–23 erg cm^{-2}. The range of values reflects the particular choice of "cratic" contributions.[4] The assignment of such values depends critically on choice of the surface of tension, normally taken at the Gibbs dividing surface. As already remarked, this is probably incorrect, and if the vander Waals boundary of the hydrocarbon is chosen, a higher value close to the bulk hydrocarbon–water interfacial energy obtains, *i.e.*, 50 erg cm^{-2}.)

Similarly, the change in electrostatic self free energy of the head group between aggregated and dispersed state is the relevant entity required. As shown in Appendix A, the capacitance form for the repulsive surface term includes only head group–head group, head group–counterion and counterion–counterion interactions; *i.e.*, we have chosen a reference state in which the head group self-energy is omitted. Although the head group in the aggregated state may have a different self-energy from that in the dispersed state due to its proximity to a region of low dielectric constant, both free energies, and therefore their difference, can be expected to be much smaller than the hydrophobic free energy change. (A very crude estimate of the electrostatic self-energy is provided by the Born expression $e^2/2\varepsilon r$. For $\varepsilon \approx 80$, $r \approx 2$ Å, we have $e^2/2\varepsilon r \approx 1.7\,kT$ while typically hydrophobic contributions to $\mu_N^0 - \mu_1^0$ amount to $\gtrsim 15\,kT$.) Hence we ignore changes in electrostatic self-energies. The interaction free energy of a head group in the dispersed state with counterions and other head groups is certainly negligible, as is evident from measured activity coefficients of salt solutions.[30]

For zwitterionic amphiphiles there will be a small additional electrostatic contribution to $\mu_N^0 - \mu_1^0$ of the form $e^2/(\varepsilon|r_+ - r_-|)$.

This completes the formulation of our model for micellar free energies, except for one caveat: to examine now the consequences of the model, the thermodynamic formulation of section 2 requires that the relation between free energy (a function of a) and the aggregation number N be spelt out. The connection between a and N is determined by the shape and size of the aggregate. For a given a, fixed hydrocarbon volume per amphiphile and aggregation number, there are geometric or packing constraints which specify the allowed shape and size. An examination of these packing constraints and their consequences will be deferred to sections 5 and 6. For the moment we shall be concerned with testing the model for the simpler problem of spherical micelles, and comparing with experiment, in order to develop confidence that the assumptions embodied in eqn (3.1) provide a satisfactory basis for prediction.

4. PRELIMINARY APPLICATION TO SPHERICAL MICELLES

To illustrate and test the viability of the model, we now consider its application to the formation of spherical micelles. In this application we ignore the important geometric constraints dealt with in the following section. These complications will be built into the theory in section 6. We consider spheres for the following reasons. If we ignore packing constraints, of all the possible shapes for aggregates, the sphere is the smallest shape with a given surface area per molecule and therefore has the lowest aggregation number. Consequently a sphere will be the thermodynamically favoured state, even in the absence of curvature corrections to electrostatic free energies, or of end-effects which will occur for rod-like micelles or planar bilayers. If curvature and end-effects are included, non-spherical shapes, *e.g.*, cylinders and bilayers, turn out to be even less favoured. Although spherical micelles are unlikely to occur in general due to packing constraints,[29, 31] restriction of the discussion to these aggregates gives us an idea of the behaviour to be expected of globular aggregates as opposed to large cylinders or bilayers. Distortions from spherical shape change the relation between area per amphiphile a and aggregation number N and this modification can be incorporated subsequently.

The thermodynamic equations of section 2 are expressed in terms of N, whereas $\mu_N^0 - \mu_1^0$ given in section 3 involves a. We need a relation between a and N. The geometry of a spherical micelle is illustrated in fig. 1 and if v denotes the volume of the hydrocarbon tail of an amphiphile we have the relations

$$N = \frac{4\pi}{3}\frac{R^3}{v} \tag{4.1}$$

and

$$a = \frac{4\pi R^2}{N} = (3v)^{\frac{2}{3}}\frac{(4\pi)^{\frac{1}{3}}}{N^{\frac{2}{3}}} = \frac{3v}{R}. \tag{4.2}$$

The first relation assumes that the density of hydrocarbon is constant in the interior of the micelle.[11] If we ignore curvature corrections the free energy per amphiphile in a micelle is from eqn (3.1) and (4.2)

$$\mu_N^0 = \gamma\left(a + \frac{a_0^2}{a}\right) + g; \qquad a_0 \equiv \sqrt{\frac{2\pi e^2 D}{\varepsilon\gamma}}. \tag{4.3}$$

Henceforth a_0 will be referred to as the optimal surface area per amphiphile, being that area at which the free energy per amphiphile in a micelle is a minimum. From eqn (2.8) the distribution of aggregates is given by

$$X_N = N\left[\frac{X_M}{M}\exp\left(-\frac{M}{kT}(\mu_N^0 - \mu_M^0)\right)\right]^{N/M}. \tag{4.4}$$

Take M to be the aggregation number at which μ_N^0 takes its optimal value, *i.e.*,

$$\mu_M^0 = 2\gamma a_0 + g, \qquad M = \frac{4\pi(3v)^2}{a_0^3}, \qquad R_M = \frac{3v}{a_0} \tag{4.5}$$

so that eqn (4.4) takes the form

$$X_N = N\left[\frac{X_M}{M}\exp\left\{-\frac{\gamma a_0 M}{kT}\left[\left(\frac{M}{N}\right)^{\frac{1}{3}} - \left(\frac{N}{M}\right)^{\frac{1}{3}}\right]^2\right\}\right]^{N/M}. \tag{4.6}$$

Note that since $a_0 = (4\pi)^{\frac{1}{3}}(3v)^{\frac{2}{3}}/M^{\frac{1}{3}}$, and the tail volume of an amphiphile is known, the only parameters which occur in the distribution eqn (4.6) are X_M, M and γ, the interfacial tension of the hydrocarbon–water interface.

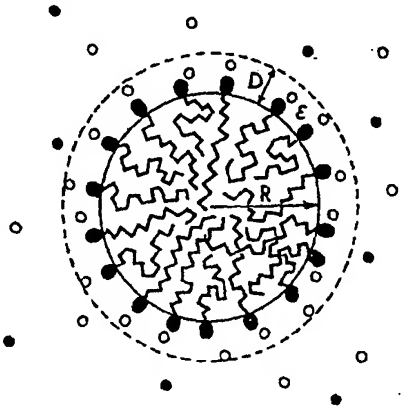

FIG. 1.—Spherical micelle.

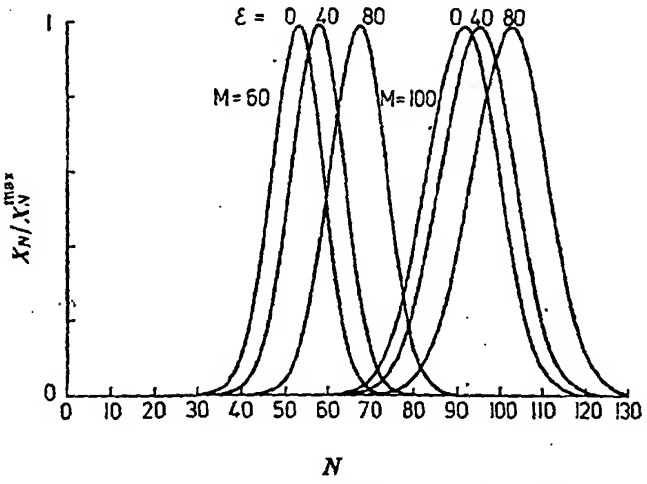

FIG. 2.—Concentration of amphiphiles X_N in spherical micelles of aggregation number N. The curves are plotted for three assumed values of dielectric constant ε. The curve for ε = 0 is equivalent to ignoring curvature corrections to the electrostatic energy. The curves are normalised to the same maximum value. X_M is taken as 10^{-4} mole fraction (5 mmol dm^{-3}).

Fig. 2 shows a plot of X_N against N for $M = 60$ and $M = 100$. For these plots v was taken to be 350 Å^3 corresponding to a hydrocarbon chain of 12 carbon atoms,[4, 11] and $\gamma = 50$ erg cm^{-2}. Several features deserve comment. The maximum of the distribution is insensitive to X_M, and therefore to total lipid concentration. The

curves are essentially Gaussians distributed about the maximum so that the mean aggregation number $\bar{N}$ and the maximum are identical. $\bar{N}$ is reduced from the optimal value M by about 10 %, so that in view of eqn (4.2) and (4.5), the area $\bar{a}$ at the maximum is only about 4 % greater than a_0, or less for higher values of M. The standard deviations of the curves are given by

$$\sigma \simeq \left(\sqrt{\frac{9kT}{2\gamma(4\pi)^{\frac{1}{3}}(3v)^{\frac{2}{3}}}}\right)M^{\frac{1}{3}} \simeq 0.4\,M^{\frac{1}{3}} \tag{4.7}$$

and the spread about the maximum is therefore a narrow one. Also, as expected from eqn (2.7) a change in lipid concentration X_M by an order of magnitude changes the mean aggregation number by only 1 or 2. These distributions are similar to those derived by Tanford.[20] The distribution does not depend on the specific form for μ_N. Any admissible form of μ_N which comes about due to a balance between opposing forces would lead to a similar distribution.

In comparing with experiment, the actual distributions are not known and are difficult to determine. What is known and available is the cmc under a range of conditions. In general, precise determinations of ln (cmc) for a given choice of parameters involve a complicated numerical routine. However, as already remarked, the system is narrowly dispersed, and can be treated to a good approximation as a monodisperse system. Further, the area $\bar{a}$ corresponding to the mean aggregation number $\bar{N}$ differs by only 4 % from the optimal area a_0. If curvature corrections to μ_N^0 are included $\bar{a}$ is shifted even closer to a_0. Thus eqn (4.3) becomes

$$\mu_N^0 = \gamma\left(a+\frac{a_0^2}{a[1+D/R]}\right)+g. \tag{4.8}$$

Since $D/R \equiv 6v\varepsilon\gamma/Me^2(M/N)^{\frac{1}{3}}$, after a little algebra, repetition of our previous analysis gives, instead of eqn (4.6), a more complicated algebraic expression involving an additional parameter ε. The corresponding distribution is plotted in fig. 2 for $\varepsilon = 80$ and 40, and we see that the net effect of curvature corrections is to shift $\bar{N}$ towards M and $\bar{a}$ towards a_0. Thus, with little error, we can take $\bar{a} = a_0$, $\bar{N} = M$, and use eqn (2.9) which becomes

$$\begin{aligned}\ln(\text{cmc}) &\simeq (2\gamma a_0+g-g')/kT \\ &= \left[\left(\frac{36\pi v^2}{M}\right)^{\frac{1}{3}}2\gamma+g-g'\right]\Big/kT \\ &\equiv \frac{K_1}{M^{\frac{1}{3}}}-K_2.\end{aligned} \tag{4.9}$$

Before we put numbers into these equations we note some qualitative predictions. Since v is roughly proportional to the number n of carbon atoms in the hydrocarbon tail, eqn (4.5) shows that ($\bar{R} \simeq R_M$) is proportional to n as observed.[32] Further, a_0 is independent of n. This is consistent with experiments on monolayers at the oil–water interface where the pressure-area isotherms are found to be insensitive to chain length above the transition area.[33] As $g'-g$ is a linear function of n, ln (cmc) is also linear in n, again as observed.[4]

The much studied sodium dodecyl sulphate (SDS) micelle provides a more substantial test. Huisman [34] measured the variation of cmc and $\bar{N}$ for these micelles as a function of NaCl concentration from 0 to 0.3 mol dm^{-3} (see also Emerson and Holtzer [35]). In eqn (4.9) all parameters except M are weakly dependent on salt concentration. Fig. 3 shows the plot of ln (cmc) against $M^{-\frac{1}{3}}$. The best fit straight

line gives $K_1 = 44$, $K_2 = 20$. With $v_{SDS} = 350$ Å^3,[4] $K_1 = 44$ implies that $\gamma \simeq 37$ erg cm^{-2}. This value, while reasonable, is somewhat less than the value 50 dyn cm^{-2} for the oil–water interface. This empirical value for γ allows an estimate to be made of the capacitance distance D. Taking $\varepsilon = 80$, D varies in the range 8 to 5 Å as salt concentration varies from 0 to 0.3 mol dm^{-3}. For smaller values of ε the values of D would be proportionately smaller. We do not place much emphasis on the magnitude of this parameter, but note that it is of the order of magnitude one would expect for the size of the Stern layer.[11] Next consider the value of $(g'-g) = K_2kT = 20\,kT \equiv 12\,000$ cal mol^{-1}. This compares with the expected hydrophobic free energy for transport of 1 CH_3 + 11 CH_2 groups from water to bulk hydrocarbon of $\sim$11 000–12 000 cal mol^{-1}.[4] If we make allowance for the area a' covered by the head group, the best fit hydrophobic energy would be reduced to $\sim$10 500 cal mol^{-1}. If in addition we admit curvature corrections this value is reduced further to $\sim$10 000 cal mol^{-1}.

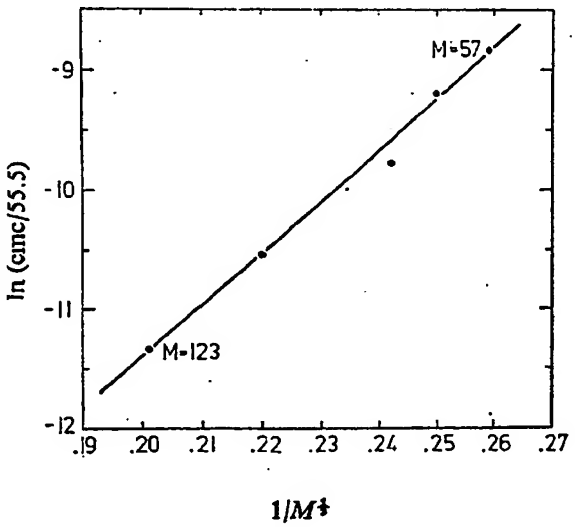

FIG. 3.—Variation of ln (cmc/55.5) with $M^{-\frac{1}{3}}$ for SDS in NaCl solutions as given by eqn (4.9). Points: experimental results. Theoretical curve is based on the assumption that the micelles are spherical. cmc/55.5 is in mole fraction units.

We could go further at this stage and check the predicted n dependence, effect of temperature on cmc, and analyse changes with salt in more detail. All of these are in good semi-quantitative agreement with experiment. To sum up: the model as developed so far gives good agreement with observation, although it might be considered that the surface free energy appears 30 % too low. However, as we cannot yet explain the existence of rod-like micelles or bilayers which suggests that geometric constraints cannot be ignored. We postpone a more precise analysis until the effects of these constraints have been investigated.

5. PACKING CONSTRAINTS AND NON-SPHERICAL MICELLES

We have already alluded to geometric limitations which place restrictions on the allowed shapes of micelles, and it is clear that packing constraints must be invoked for a proper treatment of self-assembly, for, in the absence of any such restrictions, spherical micelles will always be thermodynamically favoured over other shapes like cylindrical micelles or bilayers. There must then be some overriding factor that

forces some amphiphiles to assemble into these larger structures which appear to be thermodynamically disfavoured.

In this section therefore, we study the packing properties of amphiphiles which come about due to geometry. The most general form of the problem is exceptionally tedious because thermodynamics and packing are inextricably linked and cannot be considered in isolation. Further, the general problem of relating aggregation number to shape involves a difficult problem in the calculus of variations. Nonetheless we can make considerable progress in elucidating the role of packing provided we assume that the mean area per amphiphile will always be close to the optimum area a_0. As shown in section 4, this assumption is fair for systems which exhibit little polydispersity, and will allow us to disentangle energetic and geometric factors from the thermodynamics. This leads us to consider the shape and size of the smallest micelle consistent with $a = a_0$. This we call the critical packing shape. We shall find that beyond some characteristic critical aggregation number N_c, both spherical and ellipsoidal micelles are prohibited. Geometric factors lead us to consider different shapes once these are excluded.

Consider first a spherical micelle (fig. 1). Here the radius R, hydrocarbon core volume v and surface area a per amphiphile at the hydrocarbon–water interface are related by

$$\frac{3v}{a} = R. \tag{5.1}$$

Then, since the radius of a spherical micelle cannot exceed a certain critical length, l_c, roughly equal to but less than the fully extended length of the hydrocarbon chain, it is apparent from eqn (5.1) that once $v/a_0l_c > \frac{1}{3}$, spherical micelles will not be able to form unless the surface area $a > a_0$. This gives a critical condition for the formation of spheres:

$$\frac{v}{a_0l_c} = \frac{1}{3}. \tag{5.2}$$

On the assumption that the surface area per amphiphile is everywhere equal to or close to the optimum area a_0, we must therefore look for alternative non-spherical shapes once $v/a_0l_c > \frac{1}{3}$. (The way v and l_c are actually determined from the nature of the hydrocarbon chains is model-dependent and not of immediate concern here.) Similarly, the critical condition for cylindrical micelles and planar bilayers is readily found to be respectively

$$\frac{v}{a_0l_c} = \frac{1}{2}, \qquad \frac{v}{a_0l_c} = 1. \tag{5.3}$$

The transition shapes of amphiphilic structures, as they go from spheres to cylinders [36, 37] have not been studied; this will be our next concern.

Regardless of shape, any aggregated structure must satisfy the following two criteria: (1) no point within the structure can be farther from the hydrocarbon–water surface than l_c; (2) the total hydrocarbon core volume of the structure V and the total surface area A must satisfy $V/v = A/a_0 = N$. This criterion is only approximate since it assumes that the mean surface area per amphiphile is equal to a_0.

(a) ELLIPSOIDAL MICELLES

Tarter [31] and more recently Tanford [29] have examined the way amphiphiles can pack into prolate and oblate spheroids once they can no longer pack into spheres.

The shorter ellipsoid semi-axis was put equal to l_c and the longer axis was then determined by applying criterion (2). Both oblate and prolate ellipsoids are found to satisfy criterion (2), though for a given v, l_c and a_0 oblate spheroids have a slightly lower aggregation number N. Clearly, criteria (1) and (2) can be satisfied by many different shapes. Closer scrutiny of spheroids shows that these shapes are in fact untenable and leads us to a stronger packing condition. This can be seen as follows.

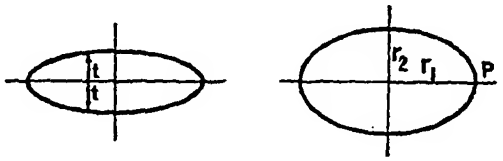

(*a*) (*b*)

FIG. 4.—Oblate spheroids.

Consider an oblate spheroid of large eccentricity [fig. 4(*a*)] satisfying criterion (2) and with minor semi-axis equal to l_c. Any local region of the oblate spheroid looks very much like a bilayer. However, for the amphiphiles to be so packed we require that $at = v$ (a constant), where $2t$ is the (varying) hydrocarbon thickness. Consequently the area per amphiphile satisfies $a \neq a_0$ almost everywhere so that the amphiphiles of the spheroid must also be energetically unfavourable almost everywhere. [Any form for the opposing surface forces will give the surface energy per unit area as constant $\times a_0 +$ constant $\times (a-a_0)^2$.] Criterion (2) disguises this energetically unfavourable situation since it contains the volume V and area A of the whole spheroid, found by averaging the amphiphile volumes and surface areas over the whole structure. By averaging the volumes and areas in this way the discrepancy in the local surface area and energy per amphiphile is averaged to zero, even though the local packing is almost everywhere energetically unfavourable. A similar situation holds for a prolate spheroid of large eccentricity. Thus criteria (1) and (2) are necessary but insufficient conditions for viable micellar structures. Another criterion is required which would indicate whether amphiphiles are packing in an energetically favourable way at all parts of an aggregate and not only on the average.

(*b*) LOCAL PACKING CRITERION

Consider an amphiphile (fig. 5) of surface area a and liquid hydrocarbon core volume v in a micelle (or bilayer vesicle) where the local radii of curvature are R_1 and R_2. Referring to fig. 5 we obtain by elementary geometry a " packing equation "

$$v/a = l\left[1-\frac{l}{2}\left(\frac{1}{R_1}+\frac{1}{R_2}\right)+\frac{l^2}{3R_1R_2}\right]; \tag{5.4}$$

where l is the length of the hydrocarbon region of the amphiphile. This equation is exact for spherical surfaces ($R_1 = R_2$), cylindrical surfaces ($R_2 = \infty$) and planar surfaces ($R_1 = R_2 = \infty$), and holds to a high degree of approximation, with an error of not more than 1 %, for surfaces of arbitrary curvature.

The weaker criteria (1) and (2) are embodied in eqn (5.4) if we stipulate that $l \leqslant l_c$. Application of eqn (5.4) to any part of a micelle or bilayer provides a test for whether or not amphiphiles there can pack in an energetically favourable way, *i.e.*, with $a = a_0$. There are no " new concepts " here; the packing equation is simply a necessary geometric expression that relates v, a, l, R_1 and R_2.

To illustrate the application of the packing equation we now show that spheroids cannot accommodate amphiphiles in their regions of greatest curvature once these amphiphiles can no longer pack into spheres, *i.e.*, once $v/a_0 l_c$ exceeds $\frac{1}{3}$. Consider the oblate spheroid of fig. 4(*b*). Since by assumption spheres are prohibited, we have $r_1 > l_c$, and by criterion (2), $r_2 \leqslant l_c$. In the region of greatest curvature P,

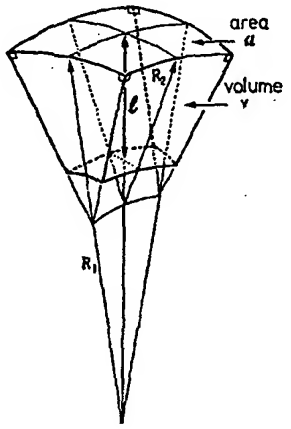

FIG. 5.—Geometric packing of a hydrocarbon region of volume v and surface area a at a surface with two radii of curvature R_1 and R_2. Eqn (5.4) gives the relation between v, a, R_1, R_2 and the length of the hydrocarbon l. For both R_1, $R_2 > l$, a void region is formed behind the hydrocarbon region.

the principal radii of curvature are $R_1 = r_1$, and $R_2 = r_2^2/r_1$, so that $R_2 < l_c$. Since $v/a_0 > l_c/3$, it is sufficient to show that v/a_0 as given by the packing equation is less than $l_c/3$. We have from eqn (5.4)

$$\frac{v}{a} = l\left[1-\frac{l}{2}\left(\frac{1}{R_1}+\frac{1}{R_2}\right)+\frac{l^2}{3R_1R_2}\right] \leqslant \frac{R_2}{2}\left(1-\frac{R_2}{3R_1}\right) \tag{5.5}$$

since l must satisfy $l \leqslant R_2$. Successive application of the inequalities $R_1 > R_2$, $R_2 < l_c$ gives further $v/a < R_2/3 < l_c/3$ which establishes the result. Thus the oblate spheroid, rather than being a viable alternative shape when amphiphiles can no longer pack into spheres, is seen to be energetically unfavourable the moment the spherical shape itself becomes unfavourable. Indeed, even when amphiphiles can pack comfortably into spheres, eqn (5.4) shows that only spheroids of low eccentricities can accommodate the amphiphiles as well. Likewise for prolate spheroids.

(*c*) PROPERTIES OF ALLOWED SHAPES

Strictly, the packing equation should be all that is needed for a complete solution of the problem of finding the shape (or shapes) that can pack amphiphiles of a given v, a_0 and l_c. However, as already remarked, the exact solution to the problem is both difficult and uncalled for. On reflection, it is apparent that the simple shape which satisfies all the packing conditions is not unlike a distorted oblate spheroid. Recall that the unacceptability of an oblate spheroid comes about because the peripheral regions had too great a curvature while the central regions were too thick. If, however, the central region is flattened so that locally it approaches a bilayer and simultaneously the curvature of the peripheral regions is reduced, the packing criteria can be satisfied. Of a number of shapes that have the general features of such a distorted oblate spheroid, a simple analytically tractable shape which satisfies all

our criteria is illustrated in fig. 7. This shape may be termed an ellipse of revolution. Qualitatively, it has the following properties: when amphiphiles can still pack into spheres the ellipse is a circle centred at the origin and the shape is therefore a sphere; as v/a_0 increases above $l_c/3$ the circle distorts into an ellipse of small eccentricity

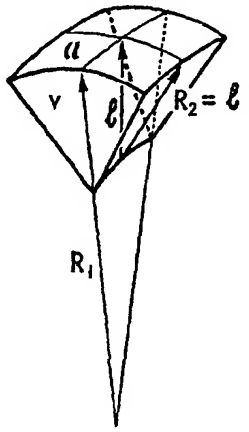

FIG. 6.—Wedge-shaped volume take up by hydrocarbon when $R_2 = l$. Note that the void region existing when $R_1 > l$ and $R_2 > l$ has disappeared (*cf.* fig. 5).

whose centre moves progressively outwards from the symmetry axis, and the micelle becomes globular. If this process were continued indefinitely, at some value of v/a_0 the shape would become toroidal-like. Ultimately, as v/a_0 approached $l_c/2$, the critical condition for cylinders, the ellipse would have become a circle once again giving an infinite cylinder.

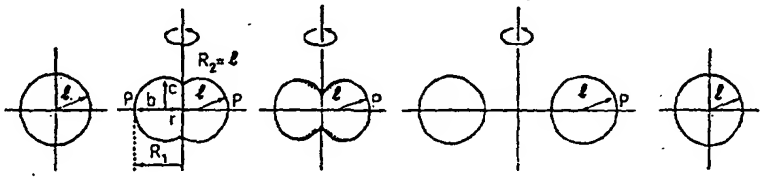

$v/a_0 l$	0.33	0.36	0.38	0.44	0.50
r/l	0	0.47	0.68	1.93	∞
b/l	1	0.72	0.70	0.85	1
c/l	1	0.85	0.84	0.92	1
$M/(4\pi l^3/3v)$	1	1.4	1.9	7.1	∞

FIG. 7.—Approximate transition shapes from spheres to cylinders, based on purely geometric considerations. For any given shape the area per amphiphile a_0 is uniform. The minimum aggregation number M is achieved at $l = l_c$ as explained in the text. More realistic transition shapes may be different due to thermodynamic requirements, discussed in section 6.

In the globular regime, *i.e.*, when micelles are still near spherical, we expect, as shown in section 4, that the distribution of sizes will be narrow, so that the approximation $a \simeq a_0$ is good; any shape which satisfies the packing criteria will be adequate here. When we come to larger aggregation numbers, we are on much more tentative ground, because the assumption of monodispersity is no longer valid, and the average micelles can be far from optimal. Indeed, when thermodynamic considerations are

involved, the initial growth phase discussed in section 6 turns out to be by a process which is in fact energetically unfavourable, through rods with spherical-like ends. Nonetheless the conclusion that large tori are energetically and geometrically favoured is a useful one, as the optimum micelle has a finite aggregation number. This is important. Otherwise, as we shall show, cylinders would continue to grow without bound, a prediction often in conflict with observation.

For completeness, we now give the equations which describe the transition micellar shapes from spheres to cylinders, and examine some of their properties.

(*d*) THE SPHERE-CYLINDER TRANSITION SHAPES

The simplest transition shape consistent with all three packing criteria are ellipses of revolution, depicted in fig. 7. The ellipse is centred at a distance r from the origin and has major and minor axes equal to c and b. At the point P, where the curvature will be a maximum, the principal radii of curvature are

$$R_1 = r+b, \qquad R_2 = c^2/b. \tag{5.6}$$

For this shape the following conditions must apply:

$$N = V/v = A/a_0 \qquad \text{[criterion (2)]} \tag{5.7}$$

$$l = R_2 = c^2/b \leqslant l_c, \tag{5.8}$$

where l the length of the hydrocarbon tail of an amphiphile at P. The assumption $l = R_2$ is not obvious. Intuitively, the reason for this choice can be seen in fig. 5 and 6. A truncated pyramid (or cone) would lead to a micelle with a region behind the hydrocarbon tail end of the amphiphile which cannot be filled up, *i.e.*, there results a micelle with a hole in it. Setting $R_2 = l$ gives instead a wedge-shaped region (fig. 6) which avoids this difficulty. The packing equation [eqn (5.4)] determines another relation of the form

$$R_1 = (r+b) = \frac{l}{3[1-2v/a_0 l]}$$

or

$$\frac{r}{b} = \frac{(c/b)^2}{3[1-2v/a_0 l]} - 1. \tag{5.9}$$

The transition shapes may be divided into a globular regime and a toroidal regime.

(*e*) GLOBULAR SHAPES ($r < b$)

For this shape we find the following expressions for the total volume V and surface area A of the hydrocarbon core:

$$V = 2\pi c[r^2 \sin\theta_0 + rb(\theta_0 + \tfrac{1}{2}\sin 2\theta_0) + b^2(\sin\theta_0 - \tfrac{1}{3}\sin^3\theta_0)] \tag{5.10}$$

$$A = 4\pi c\left[r\theta_0 + b\sin\theta_0 - \frac{[1-(b/c)^2]}{2}\left(\frac{r\theta_0}{2} - \frac{r}{4}\sin 2\theta_0 + \frac{b}{3}\sin^3\theta_0\right)\right], \tag{5.11}$$

where

$$\cos\theta_0 = -(r/b). \tag{5.12}$$

The expression for the volume V is exact, while that for the area A is approximate to first order in $[1-(b/c)^2]$, which is entirely adequate for our problem since (b/c) is

always close to 1. Applying the condition given by eqn (5.6), (5.10) and (5.11), we obtain the following equation:

$$\left(\frac{2v}{la_0}\right)\left(\frac{c}{b}\right)^2 \frac{\left[\left(\frac{[1-(b/c)^2]}{4}-1\right)\cos\theta_0 \,.\, \theta_0+\left(1-\frac{[1-(b/c)^2]}{12}(2+\cos^2\theta_0)\right)\sin\theta_0\right]}{\left[\frac{1}{3}\sin\theta_0(2+\cos^2\theta_0)-\theta_0\,.\,\cos\theta_0\right]} = 1. \tag{5.13}$$

Thus for a given value of v/a_0l, eqn (5.9), (5.12) and (5.13) may be solved to find the unique value of (b/c) from which all the other parameters such as b, c, r and N may be readily calculated. It can be seen that $N/(4\pi l^3/3v)$ is a function of v/a_0l.

(f) TOROIDAL SHAPES ($r > b$)

For this shape the total volume V and area A of the hydrocarbon core is given by:

$$V = 2\pi^2 bcr \tag{5.14}$$

$$A = 4\pi^2 cr[1-\tfrac{1}{4}[1-(b/c)^2]], \tag{5.15}$$

where again the expression for the area A is to first order in $[1-(b/c)^2]$. For this shape (b/c) is readily obtained and is given by

$$(b/c)^2 = \frac{3v/a_0l}{2-v/a_0l} \tag{5.16}$$

from which the values of b, c, r and N may be readily calculated.

For both the globular and toroidal shapes the values of N have been calculated numerically. For fixed v and a_0, N is a decreasing function of l, so that its minimum value M occurs when $l = l_c$, *i.e.*, the maximum value of l. Since we require the

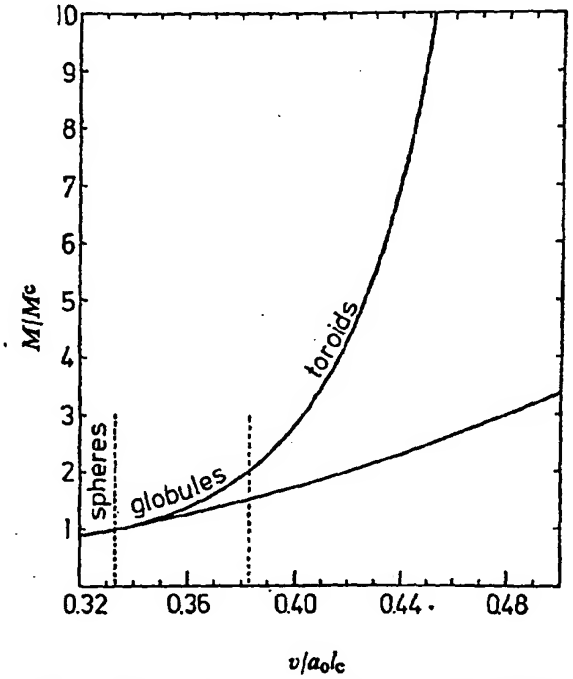

FIG. 8.—Plot of optimal aggregation number M against (v/a_0l_c) for transition shapes of the ellipsoid f revolution model. $M^c = 4\pi l_c^3/3v$ is the largest possible aggregation number for spheres consistent with packing. Lower curve corresponds to spheres with no packing constraints.

shape with the minimum aggregation number we take $l = l_c$ hereafter. The variation of $M/(4\pi l_c^3/3v)$ with $v/a_0 l_c$ is plotted in fig. 8. The range of values $v/a_0 l_c$ from $\frac{1}{3}$ to $\frac{1}{2}$ correspond to the transition from the purely spherical to the purely cylindrical shape. The results show that as $v/a_0 l_c$ increases above $\frac{1}{3}$ the spherical shape becomes progressively more globular (see fig. 7), the two radii of the ellipse become progressively smaller than l_c while the ratio b/c decreases below 1. The transition from the globular to the toroidal shape occurs when $v/a_0 l_c$ has reached 0.383 (or about 15 % higher than its value of $\frac{1}{3}$ when the spherical shape is no longer viable). At this point b/c has reached its minimum value of 0.74, and the micelle contains about twice the number of amphiphiles in a spherical micelles of the same value of v and l_c. As $v/a_0 l_c$ further decreases the toroid grows outward; both b and c increase towards l_c and the ellipse approaches a circle once more. At $v/a_0 l_c = \frac{1}{2}$, the critical condition for cylinders is reached; the ellipse is now a circle and both b and c equal l_c. For each of these shapes it may be verified that no point within the micelle is farther from the surface than l_c, and that the total curvature at the outermost regions is greater than at any other part, so that the packing equation is everywhere satisfied.

As mentioned earlier, the above model does not depend on the way v and l_c are calculated for an amphiphile. This is a separate matter, and has been analysed by Tanford,[1, 29] who used the X-ray data of Reiss-Husson and Luzzati [38] to obtain the following relations

$$\left.\begin{aligned} v &= (27.4+26.9\,n)\ \text{Å}^3 \text{ per hydrocarbon chain} \\ l_c &= (1.5+1.265\,n)\ \text{Å per hydrocarbon chain} \end{aligned}\right\}, \tag{5.17}$$

where n is some value close to but smaller than the number of carbon atoms per chain. Tanford [29] used the above relations to interpret some experimental results of Swarbrick and Daruwala [39] who measured the aggregation numbers of n-alkyl betaines in water as a function of alkyl chain length from C_8 to C_{15}. He calculated the surface area per amphiphile on the basis of an ellipsoidal model and found, somewhat unexpectedly, that this area fell considerably with increasing chain length.

TABLE 1.—AREA PER HEAD GROUP CALCULATED FOR n-ALKYL BETAINES USING PRESENT MODEL, FOR VARIOUS METHODS OF ESTIMATING v AND l_c

		$v = 27.4+26.9(n-2)$, $l_c = 1.5+1.265(n-2)$			$v = 27.4+26.9n$, $l_c = 0.8(1.5+1.265n)$	$v = 27.4+26.9n$, $l_c = 1.5+1.265n$
		Tanford [29]				
alkyl chain n	N	prolate	oblate	present model	present model	present model
C_8	24	97	95	58	70	65
C_{10}	34	92	91	59	70	66
C_{11}	58	79	77	56	67	60
C_{13}	87	74	71	56	66	59
C_{15}	130	70	66	55	65	57

Experimental values of $\bar{N}$ obtained from ref. (38).

We have repeated these calculations based on our ellipse of revolution model (see table 1), and find that the surface area is now practically invariant, *i.e.*, it is almost insensitive to chain length, as expected. We may note, too, that in Tanford's calculations, the surface areas were calculated at a distance of about 3 Å from the surface of the hydrophobic core, whereas in our calculations the surface areas were calculated at the surface of the hydrophobic core. This is consistent with our earlier conclusion (section 3) that it is at this interface that the surface area per amphiphile a_0 should be

determined, and that it is this area that should remain fairly constant with changes in curvatures and/or alkyl chain length. Our results for the n-alkyl betaines bear out this conclusion and also lend support to our micelle shape.

6. NON-SPHERICAL MICELLES: THERMODYNAMIC CONSEQUENCES OF PACKING

The thermodynamics of spherical micelle formation as discussed in section 4 provides an encouraging preliminary test of our model. We now wish to carry out a more refined comparison between experiment and theory, modified to include packing constraints. The analysis of this section falls into two parts. (1) A discussion of globular micelles. Here the model gives even better quantitative agreement with observation. (2) A discussion of the behaviour of very large aggregates. Again we compare with experiment.

(*a*) GLOBULAR MICELLES

As discussed in section 5, once aggregation numbers exceed a certain limit, it is no longer possible to pack amphiphiles into spheres. If the aggregation number is not too large, we can expect micelles to take a globular, near spherical, shape and now consider corrections to the theory which arise from this non-sphericity.

(i) CHANGES IN SALT CONCENTRATION

We proceed as in section 4, where it was shown that because the mean aggregation number $\bar{N}$ is close to the (energetically) " optimal " aggregation number M, the area per lipid is also close to a_0; the consequent error in assuming $a = a_0$ is not large.

TABLE 2

experimental results [34]			$a_0(36\pi v^2)^{\frac{1}{3}}$		
cmc/mol dm^{-3}	ln (cmc/55.5)	M	spherical approx. $1/M^{\frac{1}{3}}$	$M^c = 64$	$M^c = 57$
8.14	−8.83	57.3	0.259	0.259	0.259
5.6	−9.20	64.2	0.250	0.250	0.251
3.13	−9.78	70.8	0.240	0.243	0.245
1.47	−10.54	93.4	0.220	0.229	0.233
0.66	−11.34	123.0	0.201	0.218	0.223
$K_1 = 2\gamma(36\pi v^2)^{\frac{1}{3}}/kT$			43.5	61.5	69
γ/erg cm^2			37	52	58
K_2			20	24.5	26.5
K_2kT/kcal ($a' = 0$)			12	14.5	16
K_2kT/kcal ($a' = 20$ Å^2)			11	13	14.5

For globular micelles it would be extremely difficult to attempt a complete thermodynamic analysis. Therefore, we shall assume that the micelles are narrowly dispersed and take on the optimal size and shape discussed in section 5, *i.e.*, the shape and size of the smallest micelle which has a head group area a_0. The only consequence then of packing constraints is that the relation between a_0 and M is modified. This relation is exhibited in fig. 8. Clearly, the value one obtains for a_0 depends on what one assumes to be the largest aggregation number possible for a spherical micelle. For SDS we have taken this cut-off size (M^c) to be either one of the two smaller values 57 or 64. Were we to take $M^c > 123$ the graph of fig. 3 [in

which $a_0/(4\pi)^{\frac{1}{3}}(3v)^{\frac{2}{3}}$ is taken to be precisely $M^{-\frac{1}{3}}$] would be reproduced. The results for $M^c = 57, 64$ are tabulated in table 2 together with values of K_1, K_2 and γ which best fit the experimental data exhibited in fig. 9. K_1, K_2 are defined by

$$\ln(\text{cmc}) = [2\gamma(a_0 - a') + g - g']/kT$$
$$= K_1[a_0/(4\pi)^{\frac{1}{3}}(3v)^{\frac{2}{3}}] - K_2. \quad (6.1)$$

The best fit for $M^c = 64$ corresponds to an interfacial energy at the micelle–water interface of $\gamma = 52$ erg cm^{-2} in agreement with the measured value of γ, at the bulk oil–water interface. The interfacial energies of liquid hydrocarbon–water interfaces [13] vary from about 50 to 54 erg cm^{-2} (from section 4 with the spherical approximation, the best fit γ was 37 erg cm^{-2}). With $a' \simeq 20$ Å, the value of K_2 corresponds to a hydrophobic energy of 13 300 cal mol^{-1}. Curvature corrections (see below) reduce this to about 12 000 cal mol^{-1} close to the expected value deduced in section 4.

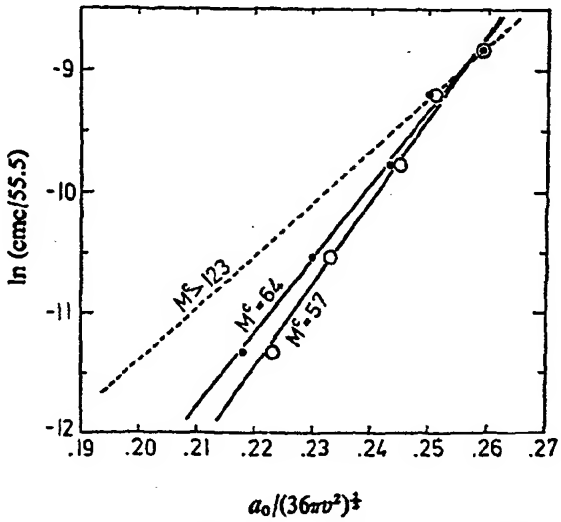

FIG. 9.—Variation of ln (cmc/55.5) with $a_0/(36\pi v^2)^{\frac{1}{3}}$ for SDS in NaCl. Data listed in table 2. ○, $M^c = 57$; ●, $M^c = 64$; - - -, $M^c > 123$ (this line ignores packing and is equivalent to fig. 3).

(ii) EFFECT OF CHANGES IN CHAIN LENGTH

Our model can be subjected to a further test. From eqn (6.1) for ln (cmc) we find that the only term which depends on n is the hydrophobic term $g - g'$. It then follows that ln (cmc) must be a linear function of n. This is found to be so experimentally. The experimental results for ln (cmc) for non-ionic surfactants or ionic surfactants at 0.5 mol dm^{-3} salt, correspond to a hydrophobic free energy [4] of about 720 cal mol^{-1} (CH_2 group)$^{-1}$. The expected hydrophobic energy as deduced from solubility data for hydrocarbons in both water and in hydrocarbon is about 820 cal mol^{-1} (CH_2 group)$^{-1}$.[4] This discrepancy can be resolved if we specialise our model to include the curvature effects discussed in section 3. Unfortunately there is some uncertainty as to the correct value of D which makes it difficult to give a proper quantitative account of curvature corrections, but we can attempt a rough accounting as follows. First, let us determine a range of values for D. We have from eqn (4.3) $a_0 = \sqrt{2\pi e^2 D/\varepsilon\gamma}$ and from table 2 we find

$$0.22 < \frac{a_0}{(4\pi)^{\frac{1}{3}}(3v)^{\frac{2}{3}}} < 0.26, \quad (6.2)$$

where for SDS [4, 11] $v = 350\,\text{Å}^3$. Whence D is in the range

$$10^{-9} < \frac{D}{\varepsilon} < 1.4\times10^{-9}\ \text{cm} \tag{6.3}$$

over the range of salt concentrations 0 to 0.3 mol dm^{-3}. Taking $\varepsilon = 40$ we have $4 < D < 5.6$ Å, and for $\varepsilon = 80$, $8 < D < 11$ Å. The first choice seems more reasonable as the choice $\varepsilon = 40$ corresponds more nearly with expectations on the dielectric constant near the oil-water interface. Now, assuming an approximately near spherical shape, the curvature correction to be added to eqn (6.1) is

$$\gamma a_0\left(\frac{1}{1+D/R}-1\right)\Big/kT = -\frac{\gamma a_0 D}{kT(R+D)}, \tag{6.4}$$

where $R \simeq 3v/a_0$ is the mean radius of the globule. This expression assumes that $a \simeq a_0$. The parameters γ, a_0, D are independent of n, and R is a linear function of n. As a typical example, take $a_0 = 60\,\text{Å}^2$ corresponding to $M^c = 64$, $\gamma = 50$ erg cm^{-2}, and $D \simeq 5$ Å. Then we obtain for various values of n using $v = 27.4+26.9\,n\,\text{Å}^3$ [eqn (5.19)], the results in table 3. It can be seen from the table that curvature corrections are in the right direction in that they reduce the hydrophobic energy and are qualitatively correct whatever choice is made for D.

TABLE 3

		$\gamma a_0 D/kT(D+R)$		difference (CH$_2$ group)$^{-1}$		difference/ cal mol^{-1} (CH$_2$ group)$^{-1}$	
n	R/Å	D = 5 Å	D = 10 Å	D = 5 Å	D = 10 Å	D = 5 Å	D = 10 Å
8	12.1	2.12	3.27				
				0.15	0.17	90	102
9	13.4	1.97	3.10				
				0.14	0.18	84	108
10	14.8	1.82	2.92				
				0.11	0.14	66	84
12	16.1	1.72	2.78				
				0.11	0.15	66	90
13	17.5	1.61	2.63				
				0.89	0.12	54	72

For alkyl sulphates in the absence of salt both D and a_0 will be larger, leading to larger curvature effects. The observed discrepancy here however is about 400 cal mol^{-1} (CH$_2$ group)$^{-1}$,[4] and this is too large a discrepancy to be accounted for by the simple capacitance model. At very low salt concentrations with ionic surfactants we expect highly non-linear behaviour for the repulsive electrostatic terms, so that this simple model can be expected to break down.

(iii) TEMPERATURE EFFECTS

We turn now to the temperature dependence of the cmc. Eqn (6.1) gives little indication of how the cmc should vary with temperature. The observed cmcs all have a minimum between 20-30°C, for sodium n-dodecyl, n-decyl and 2-decyl sulphates, and for n-dodecyl trimethylammonium bromide.[40-42] While the temperature dependence of the term $2\gamma a_0/kT$ could be estimated from data on the surface tension of water and decreases with temperature, we have no information on the temperature dependence of the hydrophobic term $g-g'$. However, evidence [4] on the solubilities and enthalpy of solution of the sequence ethane, propane, butane,

together with corresponding data for the saturated alcohols from ethanol to n-pentanol, indicates that $\partial/\partial T[(g-g')/kT]$ increases as the number n of CH_2 groups increases. Since $2\gamma a_0$ is independent of n, eqn (6.1) predicts that the slope of the cmc against T curve should increase as n increases. This qualitative prediction is in accord with Flockhart's results [40] on sodium n-alkyl sulphate micelles for $n = 10$, 12, 14.

One further prediction from eqn (6.1) is that the slope of the cmc against T curve should increase as the ionic strength increases. This follows because an increase in ionic strength causes a decrease in a_0 while other parameters in eqn (6.1) remain constant. Such an effect has been observed by Matijević and Pethica [43] with SDS micelles in 0.01-0.20 mol dm^{-3} NaCl solutions.

(*b*) ROD-SHAPED MICELLES

When a_0 is small so that the optimal size is much larger than the largest possible sphere, we have argued in section 5 that the amphiphiles would pack into large toroids if the optimal size were indeed attained. However, as can be seen from fig. 8, aggregates much smaller than the optimal may have an area per molecule, a, only marginally larger than a_0 and, consequently, self-energies μ_N^0 only marginally higher. It follows from the arguments of section 2 that in this case the system will be polydisperse and we may expect to find aggregates somewhat smaller than the optimal size. This is in contrast to the situation with globular micelles and with lipid vesicles to be discussed in the next section. The problem of determining the shape of the micelles is much more difficult. For micelles of a given aggregation number N, and, therefore, of a given volume Nv, and a given total area A, the minimum μ_N^0 can be shown to correspond to uniform area $a = A/N$, but only provided this shape is allowed by packing. The minimum μ_N^0 for the given aggregation number N would be determined by the smallest value of a. The functional relationship between this minimum area a and the given aggregation number N is the same as that between a_0 and the minimum aggregation number N illustrated in fig. 8. Use of this form leads to results which do not agree with the observed behaviour of large aggregates. However, for some values of N packing restrictions may prohibit the formation of a micelle with uniform area a, and the micelle with minimum μ_N^0 may have a non-uniform area per molecule. A possible candidate is a cylindrical micelle with $a = a_0$ having globular ends with $a > a_0$. Such a shape would have an average area per molecule very close to a_0. Experimental evidence seems to indicate that micelles of large aggregation number formed from one-tail-amphiphiles are rod-shaped.[36, 37] Such a micelle would have a μ_N^0 of the form

$$\mu_N^0 = \mu_\infty^0 + \frac{\alpha kT}{N}, \tag{6.5}$$

where μ_∞^0 is the self-energy per molecule of an infinite cylinder $= 2\gamma a_0$. The term $\alpha kT/N$ arises because the molecules in the globular ends have a larger area and the number of these is independent of N. As was shown in section 2, this form for μ_N^0 leads to very polydispersed systems whose mean aggregation number increases rapidly with amphiphile concentration, provided α is large. It is experimentally observed that the mean aggregation number of these (apparently rod-shaped) micelles does change rapidly with concentration, eventually levelling out to a fixed number.[4]

A model which might be expected to give a rough estimate of α is shown in fig. 10. Consider a cylinder of radius $r = 2v/a_0$ with spherical ends of radii l_c. Then the molecules in the hemispheres on the ends have area $a = 3v/l_c$ and all other molecules

in our model have $a = a_0$. Then if $\eta = 4\pi l_c^2/a$ denotes the number of molecules in a spherical micelle of radius l_c we find that μ_N^0 is given by

$$\mu_N^0 = 2\gamma a_0 + \eta\gamma a_0(\sqrt{a/a_0} - \sqrt{a_0/a})^2/N \tag{6.6}$$

with

$$a = 3v/l_c. \tag{6.7}$$

This gives

$$\alpha = \frac{4\pi x l_c^2 \gamma}{kT}(\sqrt{x} - 1/\sqrt{x})^2 \tag{6.8}$$

with

$$x = a_0/a = a_0 l_c/3v \tag{6.9}$$

so that x lies between 1 (corresponding to the smallest a_0 attainable by spheres) and $\frac{1}{3}$ (corresponding to the smallest a_0 attainable by infinite cylinders).

In table 4 we tabulate values of α for various values of x, assuming different values for l_c with $\gamma = 50$ erg cm^{-2}.

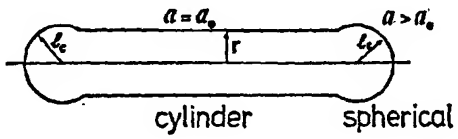

FIG. 10.—Cylindrical micelle with globular ends. Aggregation number can be less than that of the optimal torus.

TABLE 4

x	$l_c = 15$ Å α	$l_c = 25$ Å α
1	0	0
0.95	0.9	2.4
0.90	3.5	10.0
0.85	7.9	21.8
0.80	14.0	38.8
0.75	21.8	61
0.70	31.4	—
0.60	38.8	—

TABLE 5

α	$S = 10^{-10}$	$N = 2\sqrt{Sc^*}$ $S = 10^{-8}$	$S = 10^{-6}$
22	—	—	120
24	—	—	326
26	—	—	885
28	—	241	2410
30	—	654	6540
32	180	1800	1.8×10^4
34	480	4.8×10^3	4.8×10^4
36	1300	1.3×10^4	1.3×10^5
38	3000	3.6×10^4	3.6×10^5
40	10^4	10^5	10^6

Now it has already been shown in section 2 [*cf.* eqn (2.16)] that for $S \gg$ cmc and $\alpha \gg 1$, $\bar{N} = 2\sqrt{Se^{\alpha}}$ (as was obtained by Mukerjee,[44] by a different approach). In table 5 we tabulate $\bar{N}$ for various values of α at different concentrations in mole fraction units.

Some interesting features of this model deserve comment. The values of α which best fit available experimental data were found by Mukerjee [44] to lie in the range 25-35. For the amphiphiles concerned $l_c \sim$ 20-25 Å. It can be seen from tables 4 and 5 that the model used here does in fact produce values of α which straddle this range. An increase in salt concentration decreases a_0 and therefore x, so that $\bar{N}$ increases rapidly with increase in salt concentration. This is in keeping with experimental observation.[36] Also an increase in chain length increases l_c and consequently increases α. Therefore amphiphiles with larger chain lengths will tend to have micelles with larger aggregation numbers which increase faster with concentration.[4]

There is a further interesting consequence. As the lipid concentration is increased and the aggregation number is, as a consequence, increased, the " optimal size " will be approached. After this value μ_N^0 will remain constant and the micelles will cease to grow rapidly. This seems to be in keeping with experimental observation although there is some disagreement about interpretation of the results.[4, 44]

(*c*) BILAYERS

It is of interest to note here that the behaviour of lipid aggregates for which the optimal shape is a spherical vesicle or an infinite bilayer will be quite different from that of rod-shaped micelles. One might anticipate by analogy with rods that finite disc-like bilayers could form with cylindrical rims. For such a system the free energy would take the form $\mu_N^0 = \mu_\infty^0 + \alpha kT/N^{\frac{1}{2}}$. From section 2, for large α, the system will assemble spontaneously into infinite bilayers. Repetition of an analysis similar to that for rods leads to values of α sufficiently large so that this process always occurs.

7. THE STRUCTURE AND STABILITY OF ONE-COMPONENT BILAYERS

The preceding section has established that the predictions of our model accord both qualitatively and quantitatively with available observations on globular and rod-like micelles. We can, therefore, now turn with some degree of confidence to an area as yet imperfectly explored, but whose importance is not in dispute. We shall apply packing criteria to a consideration of those amphiphiles which coalesce naturally into vesicles or planar bilayers. Attention will be confined to biological phospholipids: these have anionic or zwitterionic head groups; they commonly contain two hydrocarbon chains with 16-18 carbons per chain, and display some unsaturation. It is this unsaturation that ensures that the hydrocarbon chains are above their " melting temperature ", *i.e.*, that they are in a fluid-like state, above 0°C.[4, 7, 45] Because these molecules have two hydrocarbon chains, they tend to have double the volume of the single chain molecules previously considered, for which $v/a_0 l_c \lesssim \frac{1}{3}$; thus for phospholipid molecules $v/a_0 l_c > \frac{1}{2}$, and globular and cylindrical micelles are prohibited.

We first analyse the free energy of a one-component spherical vesicle bilayer (fig. 11), and investigate its stability in the absence of packing restrictions. It should be emphasised that without packing no sensible results emerge unless we include curvature corrections. Subsequently, when packing is built into the model, curvature corrections become of secondary importance, so that the principal results do not

depend on a detailed model for the repulsive stabilising forces. In accordance with the terminology of the preceding sections, the free energy per amphiphile in a spherical vesicle of outer and inner radii R_1 and R_2 is given by

$$\mu_N^0 = \left\{4\pi(R_1^2+R_2^2)\gamma+\frac{e^2D}{2\varepsilon}\left[\frac{n_1^2}{R_1(R_1+D)}+\frac{n_2^2}{R_2(R_2-D)}\right]\right\}\Big/N \tag{7.1a}$$

$$= 4\pi\gamma\left\{(R_1^2+R_2^2)+a_0^2\left[\frac{n_1^2}{R_1(R_1+D)}+\frac{n_2^2}{R_2(R_2-D)}\right]\right\}\Big/N, \tag{7.1b}$$

where n_1 and n_2 are the number of amphiphiles in the outer and inner layers of the bilayer, e is the charge per polar head group, ε is the dielectric constant of the head group region, and D is the effective capacitor thickness of the head group. The interfacial energy of the hydrocarbon–water interface is given by γ, and the outer and inner radii, R_1 and R_2, are referred to these two hydrocarbon–water interfaces. Eqn (7.1*a*) is written in the more convenient form eqn (7.1*b*) in which the elusive parameters e, D and ε are replaced by γ and the optimum surface area per amphiphile in the bilayer a_0, as given by eqn (4.3).

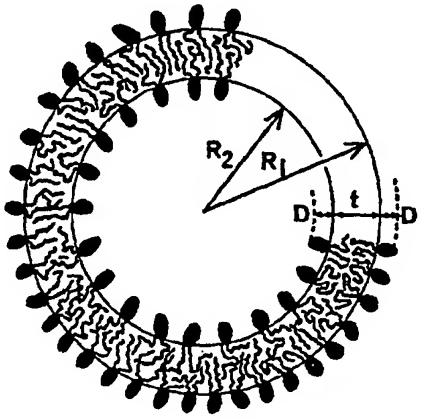

FIG. 11.—Spherical bilayer vesicle of hydrocarbon thickness t.

The aggregation number N and hydrocarbon thickness t of the vesicles are given by

$$N = n_1+n_2 = 4\pi(R_1^3-R_2^3)/v \tag{7.2}$$

and

$$t = R_1-R_2, \tag{7.3}$$

where v is the hydrocarbon volume per amphiphile, it being assumed that, to a first approximation, v is constant and independent of vesicle size. If a_1 and a_2 are the surface areas per amphiphile on the outer and inner hydrocarbon–water interfaces, we may write

$$a_1 = 4\pi R_1^2/n_1 \tag{7.4}$$

and

$$a_2 = 4\pi R_2^2/n_2. \tag{7.5}$$

Eqn (7.1)-(7.5) allow us to determine the minimum free energy configuration for a particular value of N or R_1. This is done in Appendix B where, in the absence of any packing restrictions, we obtain the following results:

$$\mu_N^0(\min) \approx 2a_0\gamma\left[1-\frac{2\pi Dt}{Na_0}\right] \tag{7.6}$$

$$a_1 \approx a_0\left[1-\frac{(R_1+3R_2)D}{4R_1R_2}\right] \tag{7.7}$$

$$a_2 \approx a_0\left[1+\frac{(3R_1+R_2)D}{4R_1R_2}\right] \tag{7.8}$$

$$t \approx \frac{2v}{a_0}\left[1+\frac{t^2}{6R_1^2}\right], \tag{7.9}$$

where a_0 is the surface area per amphiphile in the planar bilayer (*i.e.*, when $N = \infty$ or $R_1 = \infty$). From the above results we may conclude the following: (1) the minimum free energy per amphiphile is slightly lower than that in a bilayer, for which $\mu_N^0(\min) = 2a_0\gamma$. Since a spherical vesicle must have a much lower aggregation number N than a planar bilayer we conclude that spherical vesicles are thermodynamically favoured over planar bilayers and that, in the absence of any packing constraints, the vesicles will have very small radii. Indeed, if there were no packing constraints the vesicles would shrink to such a small size that they would actually form into micelles. As will be shown, packing constraints prevent vesicles from shrinking much below a certain critical packing radius. (2) The optimum area per amphiphile on the outer surface a_1 is found to be smaller than the optimum area for a bilayer a_0, while the inner area a_2 is found to be larger. (3) The hydrocarbon thickness t is slightly greater than that of a bilayer, given by $t = 2v/a_0$. For example, if $t = 30$ Å, $R_1 = 100$ Å, the value of t is increased by about 1.5 %.

While some of the above results are modified when packing constraints are introduced, the important conclusion that remains unchanged is that spherical vesicles are thermodynamically favoured over planar bilayers. The effect of packing is only to place limits on their size. We may note here that while sonication is generally employed in the laboratory for their formation this is not essential: Batzri and Korn [46] have reported the formation of vesicles without sonication. In addition, vesicles, once formed, appear to be stable for many days.[46-50] We return to this matter later.

(*a*) THE EFFECT OF PACKING CONSTRAINTS ON BILAYER STRUCTURES

In section 5, a geometric "packing equation" was derived that relates the amphiphile surface area a, hydrocarbon volume v, and hydrocarbon thickness l to the curvature at the amphiphile surface. For a spherical vesicle of outer radius R_1 the packing equation, eqn (5.4), for the outer layer amphiphiles is

$$v/a_1 = l\left[1-\frac{l}{R_1}+\frac{l^2}{3R_1^2}\right] \tag{7.10}$$

so that

$$R_1 = \frac{l[3+\sqrt{3(4v/a_1l-1)}]}{6(1-v/a_1l)}. \tag{7.11}$$

It will be shown subsequently that the thermodynamically favoured vesicles have their hydrocarbon chains maximally extended. Then $l = l_c$, and R_1 takes the minimum possible value for a given a_1. This value will be called the critical packing radius R_1^c. To a first approximation the outer amphiphile surface area a_1 may be put equal to a_0, and the value of R_1^c may then be readily obtained from eqn (7.11). As an example of

eqn (7.11) we shall use some accurately determined data [51, 52] for egg phosphatidylcholine (egg PC) for which $v = 1063\,\text{Å}^3$, $a_0 = 71.7\,\text{Å}^2$, and we obtain the following critical vesicle radii as a function of l_c. $R_1^c(l_c = 19\,\text{Å}) \approx 80\,\text{Å}$, $R_1^c(l_c = 17.5\,\text{Å}) \approx 108\,\text{Å}$, $R_1^c(l_c = 16\,\text{Å}) \approx 212\,\text{Å}$.

Before we proceed with a thermodynamic analysis it is worth considering the qualitative consequence of geometric packing in order to understand why double chained amphiphiles aggregate so differently from single chained amphiphiles. In section 5 we found, as a rule of thumb, that those amphiphiles for which v/a_0l_c lies between $\frac{1}{3}$ and $\frac{1}{2}$ form into micelles whose shapes vary gradually from spherical to cylindrical. For values of v/a_0l_c between $\frac{1}{2}$ and 1 we might expect a gradual variation from a cylindrical micelle to a planar bilayer. However, there is no way that a cylinder may be gradually distorted into a planar bilayer consistent with the geometric packing criteria. On the other hand, once the critical condition for cylinders is reached, *i.e.*, once $v/a_0l_c = \frac{1}{2}$, it may be readily verified that a very small spherical vesicle may already be packed with an outer radius R_1 equal to $(1+1/\sqrt{3})l_c \approx 1.6\,l_c$. Thus we do not need to look for a gradual transition from cylindrical micelles to bilayers. At some value of v/a_0l_c close to $\frac{1}{2}$ the spherical vesicle will become viable as regards packing, and since its aggregation number is bound to be much smaller than that of a long cylinder it will take over as the most favoured structure. As v/a_0l_c increases above $\frac{1}{2}$ the vesicle will grow, becoming a planar bilayer when v/a_0l_c reaches 1.

Tanford [4, 29] has concluded that almost all of the commonly studied amphiphiles with one hydrocarbon chain cannot pack into spherical micelles. Such amphiphiles invariably form into small globular micelles or long rod-like micelles. Thus their values of v/a_0l_c lie in the range $\frac{1}{3}$ to $\frac{1}{2}$. If the only effect of doubling the number of hydrocarbon chains is to double v/a_0l_c, we may conclude that the values of v/a_0l_c for diacyl chained phospholipids should lie in the range $\frac{2}{3}$ to 1.* By this criterion, using eqn (7.11), such phospholipids should form either planar bilayers or spherical vesicles of radii $R_1 > \sim 3l_c$.

(*b*) THERMODYNAMIC CONSEQUENCES OF PACKING CONSTRAINTS

For vesicles that are larger than the critical radius R_1, there are no packing restrictions on any of the amphiphiles and the minimum free energy configuration is given by eqn (7.5)-(7.9). Such vesicles, however, are not thermodynamically favoured over smaller vesicles which have lower aggregation numbers N. The vesicles will therefore tend to shrink; but once their outer radii become lower than the critical packing radius R_1^c, the surface areas of the outer amphiphiles a_1 must now increase above the optimal area [given by eqn (7.7)] and this increase in a_1 leads to an increased free energy per amphiphile as N or R_1 falls. We must, therefore, analyse how the free energy per amphiphile varies with N when packing constraints are included. To obtain exact solutions to the initial eqn. (7.1)-(7.4) is difficult when packing constraints, given by eqn (7.10), are introduced. But since we are concerned with vesicles where the effective capacitor length D is much smaller than the outer and inner radii R_1 and R_2 approximate solutions may be obtained by ignoring curvature effects, which are now small. This is done in Appendix B where it is first shown that the optimum surface area per amphiphile on

* As already discussed, the assumption that the surface area a_0 is not much affected by doubling the number of chains is supported by the observation that these areas are independent of chain length, and have much the same values for both single chained and double chained amphiphiles. This is also expected on theoretical grounds for hydrocarbon chains in the fluid state.

the inner surface a_2 is unaffected by the packing constraints, which, as is to be intuitively expected, only affects the outer layer amphiphiles. The inner layer amphiphiles are always in a favourable packing state; their hydrocarbon chains simply fill up the inner layer volume with their inner surface areas a_2 remaining at their optimal values, close to a_0. In Appendix B it is further shown that ignoring curvature effects the mean free energy per amphiphile is given by

$$\mu_N^0 \approx 2a_0\gamma + \frac{4\pi l_c^2\gamma}{N}(1-R_1/R_1^c)^2 \tag{7.12}$$

when R_1 is smaller than the critical packing radius R_1^c given by eqn (7.11). For $R_1 > R_1^c$ we have

$$\mu_N^0 \approx 2a_0\gamma. \tag{7.13}$$

To obtain the vesicle size distribution we substitute the above expressions into eqn (2.8). For $R_1 < R_1^c$ we obtain the following distribution law for the concentration of vesicles X_{R_1} of radius R_1:

$$X_{R_1} = N\left(\frac{X_{R^c}}{N^c}\right)^{N/N^c} \exp\{-4\pi l_c^2\gamma(1-R_1/R_1^c)^2/kT\}, \tag{7.14}$$

where N/N^c is the ratio of the aggregation numbers of vesicles with radii R_1 and R_1^c, and is given approximately by

$$N/N^c = \{R_1^2+(R_1-t)^2\}/\{(R_1^c)^2+(R_1^c-t)^2\}. \tag{7.15}$$

When $R_1 > R_1^c$ the distribution function reduces to

$$X_{R_1} = N\left(\frac{X_{R_1^c}}{N^c}\right)^{N/N^c}. \tag{7.16}$$

Eqn (7.14)-(7.16) give the concentration of vesicles as a function of R_1. As an application of this distribution we shall use the values previously obtained for egg phosphatidylcholine. Fig. 12 shows how the egg PC vesicle concentration varies with outer radius R_1 for two values of l_c and their corresponding values of R_1^c determined by eqn (7.11), *i.e.*, $l_c = 17.5$ Å, $R_1^c = 108.3$ Å, and $l_c = 16.0$ Å, $R_1^c = 212.5$ Å. We have assumed that $\gamma = 50$ erg cm^{-2}, $t = 29.6$ Å,[52] $T = 20$°C and have plotted the distributions for $(X_{R_1^c}/N^c) = 10^{-8}$ and $(X_{R_1^c}/N^c) = 10^{-14}$. The value of $(X_{R_1^c}/N^c) = 10^{-8}$ corresponds roughly to a concentration of 1 mg phospholipid per cm^3 water.

A number of general conclusions for egg PC may be drawn from the distribution.

(1) The concentration of vesicles has a near-Gaussian profile which peaks at an outer radius R_1 close to, but slightly smaller than, the critical packing radius R_1^c. At the peak, the surface area per amphiphile is slightly greater (by ~1 %) than that of the bilayer a_0, though the difference is diminished as the total amphiphile concentration increases.

(2) The profile is given approximately by $\exp\{-(R_1-R_1^c)^2/2\sigma^2\}$, where the standard deviation σ is given by

$$\sigma = \frac{R_1^c}{l_c}\sqrt{\frac{kT}{8\pi\gamma}}. \tag{7.17}$$

Thus the standard deviation σ is found to be proportional to the vesicle size R_1^c, and is approximately equal to 3 % of R_1^c. Further, the theoretical value of σ is fairly insensitive to the value chosen for the hydrocarbon–water interfacial energy γ.

(3) The mean outer radius decreases as the lipid concentration is lowered, but the magnitude of the shift is very small over a wide range of concentrations. A million-fold change in concentration shifts the peak by only a few Ångstrom units.

The implications so far are that egg PC vesicles should be fairly homogeneous in size, and that this size is effectively independent of the total amphiphile concentration even down to extremely low concentrations. In general, the factors that are expected to affect vesicle size are changes in the optimal surface area a_0 and the ratio v/l_c. For anionic amphiphiles the surface area a_0 may be expected to be changed by variations in pH, ionic strength, $[Ca^{2+}]$, *etc.*,[53] while zwitterions may be expected to be less sensitive to such changes. On the other hand, v/l_c may be expected to vary with the degree and type (*cis*, *trans*) of unsaturation.

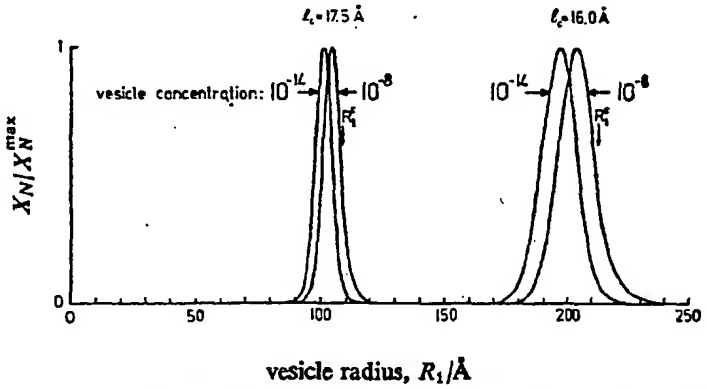

FIG. 12.—Concentration of phospholipids X_N in spherical vesicles of outer radii R_1. The curves are based on eqn (7.14)-(7.16) and are plotted for $\gamma = 50$ erg cm^{-2}, $t = 29.6$ Å (corresponding to egg PC), for two values of l_c. The vesicle concentration ($X_{R_1^c}/N^c$) is in mole fraction units (55.5 mol dm^{-3}).

We now return to fig. 12 in order to test its predictions for egg PC vesicles. These vesicles have been found experimentally [54] to have a total outer radius of 105 ± 4 Å. (A knowledge of the exact outer radius is not essential in the foregoing analysis.) Since the outer radius R_1 is measured at the hydrocarbon–water interface, a total radius of 105 Å corresponds to a value of R_1 closer to 100 Å or even less (depending on the length of the polar head group). Fig. 12 shows that for the vesicle size distribution to peak at $R_1 \approx 100$ Å requires the maximally extended hydrocarbon length to be $l_c \approx 17.5$ Å. The theoretical results also predict that the vesicle diameters will have a standard deviation of $\simeq 7$ Å, which may be compared with the experimental value of ± 8 Å,[54] and that the aggregation number (at $R_1 = 100$ Å) is 2600 as also observed.[54] Further, the ratio of the number of egg PC molecules on the outer and inner vesicle layers should be given roughly by $[R_1/(R_1 - t)]^2$, where t is the hydrocarbon thickness and not that of the whole vesicle bilayer. Putting $t = 29.6$ Å yields an outer PC/inner PC ratio of $(100/70.4)^2 = 2.0$. If instead of 29.6 Å a value of 40 Å were chosen for t (as is commonly done) we should have obtained a ratio of $(105/65)^2 = 2.6$, while for $t = 45$ Å the ratio rises to 3.1. We may note that experimental determinations of this ratio vary greatly and depend on the method of measurement. The reported values to date are: 1.6,[48] 1.7,[55] 1.85-1.95,[56-59] 2.0,[60] 2.2,[61] 2.3,[49-50] 2.6[9] (the average value is about 2.0).

As regards the outer and inner surface areas of the amphiphiles, the results indicate that these should be about the same, and close (within $\sim 1\%$) to the area in lamellar bilayers, as observed.[9, 62]

The value obtained for the maximally extended hydrocarbon length of 17.5 Å is more difficult to compare with experimental values. In section 5 we found that 80-100 % of the fully extended hydrocarbon chain appears to be a reasonable estimate of l_c of saturated chains (see also Tanford [4, 29]). Since egg PC is mainly 16 : 0, 18 : 0 and 18 : 1,[63] we obtain a theoretical estimate for l_c of $(0.8\text{-}1.0)\times[1.5+(1.265\times 16)] \approx 17.4\text{-}19.4$ Å. Alternatively, the fully extended length may be obtained from the limiting surface area at which monolayers collapse. For egg PC this occurs at a limiting area [64, 65] of 55-62 Å^2 corresponding to a fully extended hydrocarbon region (assuming $v = 1063$ Å^3) of $l_c = 17\text{-}19$ Å. (We note that the value of l_c at collapse may be somewhat greater than in the vesicle bilayer since the collapse surface area is appreciably less than the vesicle surface area. The difference is about 10 Å^2 and implies that at collapse there will be some additional hydrocarbon chain available to the interior region.)

The above conclusions appear to account fairly well for the experimentally observed behaviour of egg PC vesicles. The qualitative features of the results, however, should be generally applicable to all one-component vesicles composed of amphiphiles whose hydrocarbon chains are in a liquid-like state.

A more detailed analysis of the problem, that includes the electrostatic effects of curvature, is difficult and probably unnecessary. In section 4 the effects of curvature on micelle size were analysed and it was found that, depending on the value of the dielectric constant ε, the micelle distribution was shifted to slightly larger sizes (fig. 2). In the case of vesicles a similar result is expected. The electrostatic effect of curvature will lower the optimum area per outer amphiphile below a_0 as R_1 decreases [see eqn (7.7)]. This will shift the critical packing radius R_1^c to larger values and thereby shift the distribution curve to larger radii. On the other hand, the effect of curvature should lower the minimum energy per amphiphile as R_1 falls [see eqn (7.6)], and this will shift the distribution curve to smaller radii. These two effects will partly cancel out and the net shift could be in either direction. If, as expected, the net shift is to larger radii the implication is that l_c is slightly greater than 17.5 Å (from fig. 12 we see that a small change in l_c causes a large shift in the distribution curve).

Finally, the above analysis allows us to calculate a value for the Young's modulus of a planar bilayer under compression or tension. Rewriting the free energy per lipid, in terms of the volume v and hydrocarbon thickness t ($a = v/t$), the energy per two lipids on either side of a bilayer is $\mu_N^0 = 2\gamma(a+a_0^2/a) = 2\gamma(v/t+ta_0^2/v)$. Thus the force F on compressing the bilayer from its initial equilibrium thickness t_0 to $(t_0-\Delta t)$ is

$$\begin{aligned} F &= -\frac{\partial(2\mu_N^0)}{\partial t} = -2\gamma\left(-\frac{v}{t^2}+\frac{a_0^2}{v}\right) \\ &= \frac{2\gamma a_0}{t_0}\left(\frac{t_0^2}{t^2}-1\right) \\ &\approx 4\gamma a_0 \frac{\Delta t}{t_0^2}. \end{aligned} \tag{7.18}$$

The Young's modulus of the bilayer is therefore

$$\left.\begin{aligned} Y &= \frac{F/a_0}{\Delta t/t_0} \approx \frac{4\gamma}{t_0} \\ \text{i.e.,}\quad Yt_0 &\approx 4\gamma \approx 200 \text{ dyn cm}^{-1} \end{aligned}\right\}. \tag{7.19}$$

For a bilayer of total thickness 50 Å the effective Young's modulus is of order 4×10^8 dyn cm^{-2} when an interfacial energy of $\gamma \approx 50$ erg cm^{-2} is taken. Experimentally, it is only possible to measure Yt_0. Though experimental determinations of Y vary greatly, Requena *et al.*[66] have recently argued that the black lipid membranes have a value of Y close to 2×10^8 dyn cm^{-2}. The theoretical value of $Yt_0 \approx 200$ dyn cm^{-1} may also be compared with measured values in the range 51-357 dyn cm^{-1} for red cell membranes.[67]

We note that the elasticity discussed above is only for planar bilayers under compression or tension and does not extend to the bending of bilayers. On the contrary, our analysis has shown that the bending of a bilayer is favoured down to the critical packing radius (assuming that the lipids can freely rearrange by lateral movement and/or flip-flop), and that "bending elasticity" sets in only for radii smaller than this critical value. The elasticity of a fluid bilayer is therefore seen to be profoundly different from that of a classical elastic plate or shell.

(c) FURTHER ASPECTS OF BILAYER STRUCTURES

In general we find that, when amphiphiles aggregate, entropy favours the smallest structures, but that packing restricts the sizes and shapes of these structures. Single chained amphiphiles form small globular micelles or long rod-like micelles, whereas double chained amphiphiles form bilayers. But there are other important differences between single and double chained amphiphiles that are of some biological significance. The first is to do with the large dispersity of micellar size and aggregation number, and the great sensitivity of micellar size to changes in the total amphiphile concentration. By contrast, double chained amphiphiles form very homogeneous structures that are unaffected by the total amphiphile concentration. Further, while single chained amphiphiles have relatively high critical micelle concentrations, of order 10^{-3} mol dm^{-3}, double chained amphiphiles such as biological phospholipids, have *very low critical micelle concentrations, of order* 10^{-10} *mol dm*$^{-3}$.[4] It is these properties that make phospholipids such excellent building blocks for the formation of homogeneous and stable bilayer membranes, unaffected by drastic changes in the surrounding amphiphile concentration. However, there is always a continuous exchange of lipids with other membranes that is largely energy independent,[68, 69] and which may be important in membrane–membrane interactions.[70]

In the other extreme of very high amphiphile concentrations a very different picture emerges as bilayers (or micelles) now begin to interact with each other. We stress that our treatment applies only to dilute systems, where there are no interactions between the aggregated structures. Thermodynamically, this was expressed by putting the activity coefficient equal to unity in eqn (2.1). If such interactions are present the expressions for the free energy in both the aggregated and dispersed states will be modified by additional terms due to long range van der Waals and electrostatic interactions. Such interactions become important at high concentrations and lead to the formation of ordered mesomorphic phases.[7, 51, 52, 71-73] Our present treatment clearly does not apply to these structures, though some of the observation on mesomorphic phases have a bearing on bilayer vesicles. One of these concerns the observation that phospholipids do not always readily form into vesicles, but rather into multilamellar bilayers or myelin figures. Sonication is often, but not always, necessary to break up and transform these bilayers into vesicles. But once formed, these vesicles are homogeneous and stable, and unaffected by the length of time and intensity of sonication.[54] It seems that as soon as bulk phospholipid is placed in aqueous solution the lipids initially form into the "neat mesomorphic

phase" (*i.e.*, bilayers);[7, 51, 52, 71, 72] since as the lipids diffuse out of the bulk into the water the local lipid concentration is initially very high. Once formed, the bilayers cannot reform into vesicles without first having to break up. For this to occur, a certain activation energy must be overcome, and it is this energy that is furnished by the sonication process. But even then the total lipid concentration must be sufficiently low for the vesicles to be dilute enough not to interact significantly with each other.

Thus whereas we conclude that spherical vesicles, if allowed by packing, are thermodynamically favoured over extended bilayers, we add the reservation that they need not necessarily form spontaneously from bilayers.

It is worth examining how a vesicle might form spontaneously from a bilayer; this is shown in fig. 13. Our analysis suggests that the initial stages of the formation of a spherical bulge is energetically favourable [*cf.* eqn (7.6)], but the final stage of separation involves adhesion and fusion at the neck as the vesicle comes away from the bilayer. This often requires a certain amount of energy and brings us to the mechanism of membrane fusion which is beyond the scope of this paper.

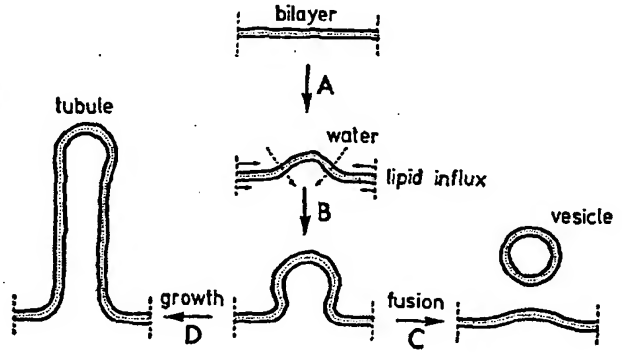

FIG. 13.—Stages of vesicle and tubule formation from a one-component bilayer. Stages A and B are energetically favourable if allowed by packing, but require free lateral diffusion of lipids in the bilayer and water flow across the bilayer. Stage C involves fusion. Stage D is energetically unfavourable for a bilayer in the fluid-state. A mechanism of vesicle and alveoli formation from a membrane similar to that shown here has been found to occur in a variety of cell types and in micropinocytosis.[74, 75]

So far we have only looked at spherical or planar bilayers. More generally, the packing equation [eqn (5.4)] shows that for a given value of a_0, v and l_c, the critical packing curvature, $\frac{1}{2}(1/R_1^c + 1/R_2^c)$, is approximately constant (where R_1^c and R_2^c are the two outer radii of a curved bilayer at critical packing). Thus for a tubular vesicle, putting $R_2^c = \infty$, its critical radius R_1^c would be about half that of a spherical vesicle. Tubular vesicles, however, have a larger aggregation number than spherical vesicles so that they should not form and they have not been reported. In addition, we show in Appendix B that the free energy per amphiphile in a tubular bilayer is higher than that in a spherical or planar bilayer. Thus we conclude that tubular protrusions should not grow spontaneously out of bilayers (fig. 13), and that bilayers in a fluid-like state should not transform into tubules. For tubular membranes to exist they must either have a resilient cytoplasmic skeleton that gives them their structure, or the membranes must be rigid. Though this conclusion may not necessarily extend to multicomponent lipid bilayers or biological membranes, we have not found any evidence for unsupported tubular membranes that are in the fluid-like state. Thus tubular cell surface projections such as filopodia, flagella, cilia and microvilli all

appear to be supported by a cytoskeleton of rigid microfilaments or microtubules.[75-82] Those tubular structures that do not have a supporting skeleton appear to have rigid (non-fluid) membraneous walls, for example, microtubules,[82] invertebrate photoreceptor membranes,[83, 84] tubular mitochondrial cristae.[75, 85, 86]

We now turn to the factors that affect vesicle properties. For anionic phospholipids, the optimum surface area a_0 may be expected to be larger at higher pH or lower ionic strength.[53] This will result in the formation of smaller vesicles, as observed for phosphatidylserine at different ionic strengths.[87]

A very different matter is to change the properties of a solvent that already contains stable vesicles in suspension, for now any changes in pH, ionic strength, $[Ca^{2+}]$, temperature, other lipid levels, *etc.*, will all induce strains on the already existent vesicles. These strains will be asymmetrical about the outer and inner faces of the vesicle bilayer,[88] and the way the vesicles will respond to these changes will depend on such factors as the flip-flop rate, the permeability of the bilayer to water and ions, and the strength and energy of rupture of the vesicle. For example, on addition of Ca^{2+} anionic vesicles are bound ultimately to rupture.[89, 90] The ruptured bilayers may then reform into larger vesicles or extended bilayers,[90] and it is probably this two-step process that the " fusion " of vesicles under the influence of Ca^{2+} occurs.[91] On the other hand the extraction of Ca^{2+} (by EDTA, for example) may cause existing vesicles to shrivel up. We have not attempted to analyse all the possibilities, though in many respects our conclusions are in agreement with our earlier model for the packing of lipids in bilayers,[92] and with the " bilayer-couple " hypothesis recently proposed by Sheetz and Singer.[93]

8. CONCLUSION

The main aim of this paper has been geared towards the building and testing of a simple model for self-assembly of ionic and zwitterionic amphiphiles. This model exists on two levels. At a non-specific level, as underlined in earlier work by Tanford,[4] the principle of opposing forces, notions concerning geometric packing properly delineated, and thermodynamics, form a framework for a model of such fundamental and general application that its predictions cannot be seriously in dispute. It is reassuring that this indeed turns out to be so, both qualitatively and quantitatively. At the level of the simple model, in dealing with comparisons of theory and experiment on micellisation, the major new point of departure in our work has been the recognition of and an attempt to quantify the role of packing. When packing constraints are recognised a number of apparently disconnected facts begin to fall into place. Thus, for globular micelles, for the effects of salt changes on cmc, the best fit occurs for an interfacial tension at the oil–water interface close to 50 dyn cm^{-1}, the known value. The rapid growth of rod-shaped micelles from globular micelles with changes of amphiphile concentration again emerges in a very natural and inevitable way once packing constraints are allowed. Further, not only do predicted parameters for the growth process agree with observation, but the packing model also predicts the observed levelling of mean aggregation number with increasing number per micelle, and the dramatic change in $\bar{N}$ with increasing chain length.

At another and more restricted level, we have imposed much more stringent requirements, as curvature effects stem from a highly specific form for the repulsive electrostatic forces. It is again reassuring, although not a necessary requirement, that such a decoration removes at least in part two sources of difficulty. These are the annoying discrepancy of 100 cal mol^{-1} $(CH_2$ group$)^{-1}$ between calculated and observed hydrophobic energies of alkane chains, and the apparent non-existence of tubular bilayer vesicles.

Especially pleasing is the circumstance that our model gives a unified framework which includes bilayers with no additional assumptions. Various physical properties of bilayer vesicles are readily accounted for. Even the Young's modulus of bilayers appears to be given correctly from elementary considerations.

As far as simple modelling of self-assembly is concerned, the treatment of single component lipid molecules given here has probably been pushed as far as it can. The refinement of our theory of self-assembly requires a proper examination of Stern layers, consequences of deviations from liquid-like properties of hydrocarbon chains,[94] head group steric effects, specific ion adsorption and other effects. While such a more rigorous analysis would undoubtedly provide specific insights into the properties of particular molecules, it is doubtful if a more refined theory will provide a better overview.

The simple model does allow an entry point into the study of self-assembly of multicomponent lipid systems, lateral phase separation (clustering), membrane asymmetry, and in particular how these relate to curvature through packing. These form a central class of problems in membrane biology.

This work arose from some earlier unpublished ideas of Dr. L. R. White and one of us (J. N. I.), which were presented at the 49th National Colloid Symposium, Potsdam, N.Y., in 1975.

APPENDIX A

ELECTROSTATIC ENERGY OF ZWITTERIONIC ARRAYS

We give here an example which illustrates how the capacitance form for the electrostatic interaction energy comes about for the special case of zwitterionic head groups.

Consider a planar lattice of parallel "dipoles" oriented normal to the plane. The positive and negative charges of each "dipole" representing a zwitterionic head group are separated by a distance D, and the array is immersed in a medium of dielectric constant ε. Let a denote the area of an elementary cell of the lattice, *i.e.*, the area per dipole. The electrostatic interaction energy per dipole is then

$$u_{el} = -\frac{e^2}{\varepsilon}\left[\frac{1}{D} + \sum_{m,n=-\infty}^{\infty}{}' \left(\frac{1}{(r^2+D^2)^{\frac{1}{2}}} - \frac{1}{r}\right)\right], \tag{A1}$$

where r denotes the position vector of a dipole relative to a fixed dipole and the sum ranges over the whole lattice excluding the reference dipole ($m = n = 0$). For a square lattice $r = |r| = \sqrt{(m^2+n^2)a}$. We see immediately that $u_{el} = e^2/\varepsilon D \times$ a function of $D/\sqrt{a}$. In the limit $D \to 0$, u_{el} reduces to the energy of a lattice of point dipoles of dipole moment eD. We are concerned with the opposite limiting case $D/\sqrt{a} \to \infty$, and first obtain the leading asymptotic term, which follows quite easily. Taking Mellin transforms [95] with respect to D, and inverting, we can estimate the integral representation

$$\frac{1}{(r^2+D^2)^{\frac{1}{2}}} - \frac{1}{r} = \frac{1}{4\pi i}\int_\gamma \left(\frac{r}{D}\right)^s \Gamma\left(\tfrac{s}{2}\right)\frac{\Gamma(\frac{1}{2}-s/2)}{\Gamma(\frac{1}{2})}\,ds, \tag{A2}$$

where the contour of integration is a line parallel to the imaginary axis which satisfies $-2 < \mathrm{Re}\, s < 0$. This integral representation can be substituted into eqn (A1) and the summation and integration interchanged provided we now choose γ such that

$-2 < \mathrm{Re}\, s < -1$, since the sum Σr^{s-1} converges when $\mathrm{Re}\, s < -1$. Thus we obtain

$$u_{el} = -\frac{e^2}{\varepsilon}\left[\frac{1}{D} + \frac{1}{4\pi i}\int_\gamma D^{-s}\,\frac{\Gamma()\Gamma^2(\frac{1}{2}-\frac{s}{2})}{\Gamma(\frac{1}{2})}\sum r^{s-1}\,ds\right]. \tag{A3}$$

The asymptotic form of u_{el} as $D \to \infty$ is now given by the residue at the pole $s = -1$. To evaluate the residue we observe that the sum Σr^{s-1} has the same singularity as the integral

$$\frac{1}{a}\int |r|^{s-1}\,\mathrm{d}^2 r \sim \frac{2\pi/a}{(s+1)}.$$

Evaluating the residue of the integrand of eqn (A3) at the pole $s = -1$, we have

$$u_{el} \underset{(D\to\infty)}{\sim} \frac{2\pi e^2 D}{\varepsilon a}. \tag{A4}$$

The above argument does not depend on the assumption that the dipoles lie on a lattice since only the residue of the sum Σr^{s-1} at its pole at $s = -1$ comes into the final answer, and this will be the same even if the dipoles are irregularly distributed so long as they have an average density $1/a$. Indeed, if we consider the correlation energy of a statistical distribution of dipoles we have

$$u_{el} = -\frac{e^2}{\varepsilon}\left[\frac{1}{D} + \frac{1}{a}\int g(r)\,\mathrm{d}^2 r\left(\frac{1}{(r^2+D)^{\frac{1}{2}}} - \frac{1}{r}\right)\right], \tag{A5}$$

where $g(r)$ is the radial distribution function (which tends to unity as $r \to \infty$). This expression leads to the same asymptotic form eqn (A4), and since the asymptotic result is linear in the coupling constant e^2, so, therefore, will be the free energy.

To establish the range of validity of eqn (A4) we need further terms in a complete asymptotic expansion. This is a more difficult problem and to derive such expansions we return to eqn (A3). The sum can be carried out exactly [96] in terms of known transcendental functions to give

$$\sum r^{s-1} = \sum_{m,n=-\infty}^{\infty}{}' \frac{(\sqrt{a})^{s-1}}{(m^2+n^2)^{(1-s)/2}} = 4(\sqrt{a})^{s-1}\,\zeta\left(\frac{1}{2}-\frac{s}{2}\right)\beta\left(\frac{1}{2}-\frac{s}{2}\right), \tag{A6}$$

where $\zeta(z)$ is the Riemann zeta function, and $\beta(z)$ is a related entire function [96] defined for $\mathrm{Re}\, z > 1$ as

$$\beta(z) = \sum_{n=0}^{\infty}\frac{(-1)^n}{(2n+1)^z}. \tag{A7}$$

The properties of $\beta(z)$ are enumerated in the important paper of Glasser.[96] Thus

$$u_{el} = -\frac{e^2}{\varepsilon}\left[\frac{1}{D} + \frac{2}{2\pi i\sqrt{a}}\int_\gamma\left(\frac{D}{\sqrt{a}}\right)^{-s}\frac{\Gamma(\frac{s}{2})\Gamma(\frac{1}{2}-s/2)}{\Gamma(\frac{1}{2})}\,\zeta\left(\frac{1}{2}-\frac{s}{2}\right)\beta\left(\frac{1}{2}-\frac{s}{2}\right)\right] \tag{A8}$$

with $-2 < \mathrm{Re}\, s < -1$. Translating the contour to the right we have poles at $s = -1$ with residue (-2) from the zeta function, a pole of $\Gamma(s/2)$ at $s = 0$ with residue $(+2)$ and a pole at $s = 1$ with residue (-2) due to $\Gamma(\frac{1}{2}-s/2)$, and find

$$u_{el} = \frac{e^2}{\varepsilon}\left[\frac{2\pi D}{a} + \frac{4}{\sqrt{a}}\,\zeta(\tfrac{1}{2})\,\beta(\tfrac{1}{2}) - \frac{4}{2\pi i\sqrt{a}}\int_{c-i\infty}^{c+i\infty}\left(\frac{2D\pi}{\sqrt{a}}\right)^{-s}\Gamma(s)\,\zeta\left(\frac{1}{2}+\frac{s}{2}\right)\beta\left(\frac{1}{2}+\frac{s}{2}\right)ds\right]; \tag{A9}$$

$$1 < c$$

To obtain this expression, note that the contribution from the pole at $s = 1$ cancels with the term in $1/D$ in eqn (A8). We have also used the Riemann relation [97] linking $\zeta(s)$ with $\zeta(1-s)$, a corresponding relation [96] for $\beta(s)$ and the duplication formula for the gamma function.[97] If we now use eqn (A6) again the last integral can be easily re-expressed as a sum, and since $\zeta(\frac{1}{2}) = -1.460$, $\beta(\frac{1}{2}) = 0.6677$,[96] we have

$$u_{el} = \frac{2\pi De^2}{\varepsilon a}\left[1-\frac{0.6206\sqrt{a}}{D}-\frac{\sqrt{a}}{2\pi D}\sum_{m,n=-\infty}^{\infty}{}' \frac{1}{(m^2+n^2)^{\frac{1}{2}}}\exp\left\{-\frac{2\pi D}{\sqrt{a}}\sqrt{m^2+n^2}\right\}\right]. \quad \text{(A10)}$$

Note that if $D \gtrsim \sqrt{a}$, the sum converges with extreme rapidity and can be ignored, so that to sufficient approximation

$$u_{el} \underset{(D/\sqrt{a}\gtrsim 1)}{\simeq} \frac{2\pi De^2}{\varepsilon a}\left[1-\frac{0.62\sqrt{a}}{D}\right]. \quad \text{(A11)}$$

For small $D/\sqrt{a}$, the corresponding expansion follows directly from eqn (A8) and gives

$$u_{el} \simeq -\frac{e^2}{\varepsilon}\left[\frac{1}{D}-\frac{2D^2\,\zeta(\frac{3}{2})\,\beta(\frac{3}{2})}{a^{\frac{3}{2}}}+O\left(\frac{D^3}{a^2}\right)\right], \quad \text{(A12)}$$

where $\zeta(\frac{3}{2}) = 2.612$, $\beta(\frac{3}{2}) = 0.864$.

These techniques can also be developed further to deal with Stern layer problems. Note that for $D \simeq \sqrt{a}$, the "effective" capacitance distance D is reduced by a factor $(1-0.62\sqrt{a}/D)$. If image effects are included, it can be shown that (when the zwitterions are immersed in a high dielectric medium $\varepsilon = 80$, adjacent to a hydrocarbon surface $\varepsilon = 2$), image effects can virtually double the electrostatic energy so that the two effects may partially cancel out. Nonetheless the observation that u_{el} is reduced from the intuitive capacitance form is of some interest, as it is known [4] that for ionic micelles use of Debye–Hückel theory (at low salt equivalent to the capacitance form) gives results for the repulsive free energy too large by a factor of 2.

APPENDIX B

(1) MINIMUM FREE ENERGY FOR VESICLES

We outline here the steps necessary to derive the results quoted in section 7.

(*a*) SPHERICAL VESICLES: NO PACKING CONSTRAINTS

Consider first a spherical vesicle comprising N amphiphiles. The free energy of the vesicle is

$$G \equiv N\mu_N^0 = 4\pi\gamma(R_1^2+R_2^2)+\frac{1}{2}\frac{n_1^2e^2D}{\varepsilon R_1(R_1+D)}+\frac{1}{2}\frac{n_2^2e^2D}{\varepsilon R_2(R_2-D)}, \quad \text{(B1)}$$

where R_1, n_1 ; R_2, n_2 refer to outer and inner surfaces. When packing is ignored, the only constraints are those due to conservation of volume and number, *viz*

$$Nv = \frac{4\pi}{3}(R_1^3-R_2^3) \quad \text{(B2)}$$

$$N = n_1+n_2. \quad \text{(B3)}$$

Since N is fixed, there are only two variables which can be taken as n_1, R_1. Then

n_2 and R_2 are determined. We first minimise G with respect to n_1, taking R_1, R_2 constant. This gives

$$\frac{\partial G}{\partial n_1} = \frac{e^2 D}{\varepsilon}\left\{\frac{n_1}{R_1(R_1+D)} - \frac{n_2}{R_2(R_2-D)}\right\} = 0. \tag{B4}$$

Physically this condition is equivalent to the statement that there is no potential difference across the vesicle in a situation of minimum free energy. Using eqn (B3) and (B4) we have

$$\min_{n_1} G = 4\pi\gamma(R_1^2+R_2^2) + \frac{1}{2\varepsilon}\frac{N^2 e^2 D}{R_1^2+R_2^2+(R_1-R_2)D}. \tag{B5}$$

We now minimise with respect to the remaining variable R_1, using $\partial R_2/\partial R_1 = R_1^2/R_2^2$, which follows from eqn (B2). The condition for a minimum is

$$\frac{\partial}{\partial R_1}(\min_{n_1} G) = 0 \tag{B6}$$

or, after a little algebra

$$\left(\frac{4\pi}{N}(R_1^2+R_2^2)\right)^2 = \frac{2\pi e^2 D}{\varepsilon\gamma}\frac{\left[1-(R_1-R_2)\dfrac{D}{2R_1R_2}\right]}{\left[1+(R_1-R_2)\dfrac{D}{(R_1^2+R_2^2)}\right]}. \tag{B7}$$

This equation can be solved by iteration as follows: clearly, for $R_1, R_2 \gg D$ there is only one solution. The first approximation can be found by dropping terms in D inside the square brackets. This gives

$$\bar{a}^2 \equiv \left(\frac{4\pi(R_1^2+R_2^2)}{N}\right)^2 = \frac{2\pi e^2 D}{\gamma} \tag{B8}$$

or $a_1 = a_2 = a_0$. To find the second approximation to the solution of eqn (B7), we find solutions R_1, R_2 of the equations

$$\begin{aligned} 4\pi(R_1^2+R_2^2) &= Na_0 \\ \frac{4\pi}{3}(R_1^3-R_2^3) &= Nv. \end{aligned} \tag{B9}$$

These approximate values can then be substituted inside the square brackets of eqn (B7) to yield a better value for $R_1^2+R_2^2$ on the left side. Writing $t = R_1-R_2$, the solution of eqn (B9) is

$$t = \frac{2v}{a_0}\left(1+\frac{t}{6R_1^2}+O(t^3)\right) \simeq \frac{2v}{a_0}\left(1+\frac{16\pi v^2}{3Na_0^3}\right) \tag{B10}$$

$$R_1 = \left\{t+\sqrt{\frac{Na_0}{2\pi}-t^2}\right\}\Big/2, \qquad R_2 = R_1-t. \tag{B11}$$

Substitution of these values into eqn (B7) then gives the average area $\bar{a}$ to second approximation

$$\bar{a}^2 = a_0^2\left\{1-\frac{tD}{\left(\dfrac{Na_0}{4\pi}-t^2\right)}\right\}\Big/\left(1+\frac{4\pi tD}{Na_0}\right). \tag{B12}$$

Optimal areas a_1, a_2 are now given as

$$a_1 = \frac{4\pi R_1^2}{n_1} = a_0\left\{1-\frac{D(R_1+3R_2)}{4R_1R_2}\right\}$$
$$a_2 = \frac{4\pi R_2^2}{n_2} = a_0\left\{1+\frac{D(3R_1+R_2)}{4R_1R_2}\right\}. \tag{B13}$$

The minimum free energy is now from eqn (B5)

$$G_{\min} = N\gamma\left[\bar{a}+\frac{a_0^2}{\bar{a}\left(1+\frac{4\pi D(R_1-R_2)}{N\bar{a}}\right)}\right]$$
$$= 2N\gamma a_0 - 4\pi\gamma Dt, \tag{B14}$$

where t is given by eqn (B10).

(*b*) CRITICAL RADIUS

Let l_c be the maximum extended length of a lipid molecule. As N decreases we eventually reach a critical radius below which packing constraints become important. This radius R_1^c is determined by

$$n_1 v = \frac{4\pi R_1^2}{a_1} v = \frac{4\pi}{3}[R_1^3-(R_1-l_c)^3] \tag{B15}$$

with a_1 given by (B13). To a sufficient approximation $a_1 \approx a_0$ (B15) becomes

$$l_c = \frac{v}{a_0}\left[1+\frac{v}{a_0R_1^c}+\frac{5}{3}\left(\frac{v}{a_0R_1^c}\right)^2+\ldots\right]. \tag{B16}$$

Eqn (B15) determines R_1^c and is a special case of eqn (5.4).

(*c*) PACKING CONSTRAINTS

Now suppose that $N < N^c$. We wish to find the configuration of such a vesicle with minimum free energy. The additional constraint is now eqn (B15), and for fixed N, l_c the free energy involves only a single variable. Note now that we must have a potential across the membrane. It is convenient here to rewrite eqn (B1) in the form

$$G = n_1\gamma\left(a_1+\frac{a_0^2}{a_1}\right)+n_2\gamma\left(a_2+\frac{a_0^2}{a_2}\right), \tag{B17}$$

where we have ignored curvature corrections to the electrostatic contribution to a first approximation. A complete solution to the problem of minimising this function is very difficult and we proceed as follows: we first show that $\partial a_2/\partial a_1 \gg 1$. This follows from the constraints

$$\frac{4\pi}{3}(R_1^3-R_2^3) = Nv \Rightarrow \frac{\partial R_2}{\partial R_1} = \frac{R_1^2}{R_2^2}$$
$$\frac{4\pi}{3}[R_1^3-(R_1-l_c)^3] = n_1 v \Rightarrow \frac{\partial n_1}{\partial R_1} = \frac{4\pi l_c}{v}(2R_1-l_c)$$
$$n_1+n_2 = N \Rightarrow \frac{\partial n_2}{\partial R_1} = -\frac{4\pi l_c}{v}(2R_1-l_c)$$

$$\frac{4\pi R_1^2}{n_1} = a_1 \Rightarrow \frac{\partial a_1}{\partial R_1} = 4\pi\left\{\frac{2R_1}{n_1} - \frac{R_1^2}{n_1^2}\frac{\partial n_1}{\partial R_1}\right\}$$
$$= \frac{8\pi R_2}{n_1}\left\{1 - \frac{2\pi R_1 l_c}{n_1 v}(2R_1 - l_c)\right\}$$
$$\frac{4\pi R_2^2}{n_2} = a_2 \Rightarrow \frac{\partial a_2}{\partial R_1} = 4\pi\left\{\frac{2R_1^2}{n_2 R_2} + \frac{4\pi R_2^2 l_c}{n_2^2 v}(2R_1 - l_c)\right\}$$
$$= \frac{8\pi R_2}{n_2}\left\{\frac{R_1^2}{R_2^2} + \frac{2\pi R_2 l_c}{n_2 v}(2R_1 - l_c)\right\}.$$

Hence

$$\frac{\partial a_2}{\partial a_1} = \frac{\partial a_2}{\partial R_1}\Big/\frac{\partial a_1}{\partial R_1} = \frac{n_1^2 R_2^2}{n_2^2 R_1^2}\frac{\left\{\frac{n_2 R_1^3}{n_1 R_2^3} + \frac{2\pi R_1 l_c}{n_1 v}(2R_1 - l_c)\right\}}{\left\{1 - \frac{2\pi R_1 l_c}{n_1 v}(2R_i - l_c)\right\}}. \tag{B18}$$

Now from eqn (B15)

$$\frac{2\pi R_1 l_c}{n_1 v}(2R_1 - l_c) = \frac{4\pi R_1^2 l_c}{n_1 v}\left(1 - \frac{l_c}{2R_1}\right) = \frac{a_1 l_c}{v}\left(1 - \frac{l_c}{2R_1}\right) \simeq \left(1 + \frac{l_c}{2R_1}\right). \tag{B19}$$

Hence (B18) becomes

$$\left|\frac{\partial a_2}{\partial a_1}\right| \gtrsim \frac{n_1 R_1}{n_2 R_2}\left(\frac{2R_1}{l_c}\right) \simeq \frac{2R_1^4}{R_2^3 l_c} \gg 1. \tag{B20}$$

Typically for egg PC, $R_1 \sim 100$ Å, $R_2 \sim 70$ Å, $l_c \sim 17$ Å, $|\partial a_2/\partial a_1| > 30$. Consequently [*cf.* eqn (B17)] a small change in a_1 produces a dramatic increase in a_2 and therefore in G. Thus we can conclude that when G is near its minimum value $a_2 \simeq a_0$, and after rewriting (B17) in the form

$$G = 2N\gamma a_0 + \frac{n_1\gamma(a_1 - a_0)^2}{a_1} + \frac{n_2\gamma(a_2 - a_0)^2}{a_2} \tag{B21}$$

we may ignore the term in n_2. Thus $G = 2N\gamma a_0 + n_1\gamma a_1(1 - a_0/a_1)^2$. From (B15), (B16)

$$\frac{a_0}{a_1} \approx \frac{1 - l_c/R_1}{1 - l_c/R_1^c} \approx 1 - \frac{l_c}{R_1}\left(1 - \frac{R_1}{R_1^c}\right).$$

Hence

$$G \approx 2N\gamma a_0 + \frac{n_1\gamma a_1 l_c^2}{R_1^2}\left(1 - \frac{R_1}{R_1^c}\right)^2$$
$$\approx 2N\gamma a_0 + 4\pi\gamma l_c^2\left(1 - \frac{R_1}{R_1^c}\right)^2. \tag{B22}$$

The corrections to this result due to curvature can, to the lowest approximation, be computed ignoring packing, and added to (B22).

(2) TUBULAR VESICLES

Consider now a tubular vesicle. We shall show that the free energy per lipid of such an assembly is greater than that for a bilayer, so that tubular vesicles will not

form, being disfavoured both energetically and entropically. To do this, it is not necessary to deal with the more difficult problem which includes complications due to packing. In the capacitance model for the repulsive forces, the free energy per unit length of a tubular vesicle is

$$\frac{G}{L} = 2\pi\gamma(R_1+R_2)+\frac{n_1^2e^2}{\varepsilon}\ln\left(\frac{R_1+D}{R_1}\right)-\frac{n_2^2e^2}{\varepsilon}\ln\left(\frac{R_2-D}{R_2}\right) \tag{B23}$$

where R_1, R_2 are outer and inner radii, n_1, n_2 denote number of head groups per unit area. For a given aggregation number N per unit length, the constraint equations corresponding to eqn (B2), (B3) are

$$N = n_1+n_2, \qquad \pi(R_1^2-R_2^2) = Nv. \tag{B24}$$

Again we take n_1, R_1 as the two independent variables, and first minimise with respect to n_1 and fixed R_1 remembering that $n_1+n_2 = N$. This gives

$$\min_{n_1}\left(\frac{G}{L}\right) = 2\pi\gamma(R_1+R_2)+\frac{Nn_1e^2}{\varepsilon}\ln\left(\frac{R_1+t}{R_1}\right). \tag{B25}$$

Now, minimising with respect to R_1 we find

$$\frac{G}{L}\min = \min_{R_1}\left\{\min_{n_1}\left(\frac{G}{L}\right)\right\} = 2\pi\gamma(R_1+R_2)+ \frac{N^2e^2}{\varepsilon}\left\{\frac{\ln\left(\frac{R_1+t}{R_1}\right)\ln\left(\frac{R_2}{R_2-t}\right)}{\ln\left(\frac{R_1+t}{R_1}\right)+\ln\left(\frac{R_2}{R_2-t}\right)}\right\}. \tag{B26}$$

It is now straightforward to demonstrate that the optimal free energy per lipid G/NL (min) satisfies

$$\frac{G}{NL}(\min) > \gamma\left[a+\frac{a_0^2}{a}\left(1+\frac{D^2}{12R_1R_2}\right)\right] > 2\gamma a_0. \tag{B27}$$

If the packing constraints are included the free energy per lipid would be even larger than $2\gamma a_0$, the optimal energy for a bilayer. Hence we conclude that tubular vesicles can not exist, *i.e.*, that planar or spherical bilayers are the preferred assembly.

[1] V. A. Parsegian, *Ann. Rev. Biophys. Bioeng.*, 1973, 2, 221.
[2] D. G. Hall and B. A. Pethica, in *Nonionic Surfactants*, ed. M. J. Schick (Marcel Dekker, New York, 1967).
[3] T. L. Hill, *Thermodynamics of Small Systems* (W. A. Benjamin, New York, 1964), vol 2.
[4] C. Tanford, *The Hydrophobic Effect* (John Wiley & Sons, New York, 1973).
[5] M. J. Lighthill, *Fourier Analysis and Generalized Functions* (Cambridge University Press, London, 1970).
[6] G. N. Watson, *Treatise on the Theory of Bessel Functions* (Cambridge University Press, London, 1966).
[7] R. M. Williams and D. Chapman, *Progr. Chem. Fats and Other Lipids*, 1970, 11, 3.
[8] Y. K. Levine and M. H. F. Wilkins, *Nature NB*, 1971, 230, 69.
[9] E. G. Finer, A. G. Flook and H. Hauser, *Biochim. Biophys. Acta*, 1972, 260, 49.
[10] A. Wishnia, *J. Phys. Chem.*, 1963, 67, 2079.
[11] D. Stigter, *J. Colloid Interface Sci.*, 1967, 23, 379.
[12] F. M. Fowkes, *J. Phys. Chem.*, 1972, 66, 382.
[13] J. F. Padday and N. D. Uffindell, *J. Phys. Chem.*, 1968, 72, 1407.
[14] *Handbook of Chemistry and Physics*, ed. R. C. Weast (Chemical Rubber Co., Ohi , 1971).
[15] R. B. Hermann, *J. Phys. Chem.*, 1972, 76, 2754.

[16] J. A. Reynolds, D. B. Gilbert and C. Tanford, *Proc. Nat. Acad. Sci. U.S.A.*, 1974, **71**, 2925.
[17] R. C. Tolman, *J. Chem. Phys.*, 1949, **17**, 333.
[18] D. S. Choi, M. S. Jhon and H. Eyring, *J. Phys. Chem.*, 1970, **53**, 2608.
[19] C. Tanford, *J. Phys. Chem.*, 1974, **78**, 2469.
[20] C. Tanford, *Proc. Nat. Acad. Sci.*, 1974, **71**, 1811.
[21] D. Stigter, *J. Phys. Chem.*, 1975, **79**, 1008, 1015.
[22] P. Debye, *J. Phys. Colloid Chem.*, 1949, **53**, 1.
[23] P. Mukerjee, *J. Phys. Chem.*, 1969, **73**, 2054.
[24] Y. Ooshika, *J. Colloid Sci.*, 1954, **9**, 254.
[25] A. Veis and C. W. Hoerr, *J. Colloid Sci.*, 1960, **15**, 427.
[26] D. C. Poland and H. A. Scheraga, *J. Colloid Interface Sci.*, 1966, **21**, 272.
[27] M. C. Phillips, E. G. Finer and H. Hauser, *Biochim. Biophys. Acta*, 1972, **290**, 397; H. Hauser, personal communication, and presented at the 49th National Colloid Symposium (Potsdam, N.Y., 1975).
[28] D. A. Cadenhead, R. J. Demchak and M. C. Phillips, *Kolloid-Z.*, 1967, **220**, 59.
[29] C. Tanford, *J. Phys. Chem.*, 1972, **76**, 3020.
[30] R. A. Robinson and R. H. Stokes, *Electrolyte Solutions* (Butterworth, London, 2nd edn., 1959).
[31] H. V. Tartar, *J. Phys. Chem.*, 1955, **59**, 1195.
[32] A. E. Alexander and P. Johnson, *Colloid Science* (Clarendon Press, Oxford, 1950), chap. 34.
[33] J. Mingins and J. A. G. Taylor, *Proc. Roy. Soc. Med.*, 1973, **66**, 383; J. Mingins, personal communication.
[34] J. F. Huisman, *Thesis* (Utrecht, 1964). Data also given in M. J. Sparnaay, *The Electrical Double Layer* (Pergamon, New York, 1972), p. 232.
[35] M. F. Emerson and A. Holtzer, *J. Phys. Chem.*, 1967, **71**, 1898.
[36] K. Kalyanasundaram, M. Grätzel and J. K. Thomas, *J. Amer. Chem. Soc.*, 1975, **97**, 3915.
[37] P. Debye and W. Anacker, *J. Phys. Colloid Chem.*, 1951, **55**, 644.
[38] F. Reiss-Husson and V. Luzzati, *J. Phys. Chem.*, 1967, **71**, 957.
[39] J. Swarbrick and J. Daruwala, *J. Phys. Chem.*, 1970, **74**, 1293.
[40] B. D. Flockhart, *J. Colloid Sci.*, 1961, **16**, 484.
[41] G. Pilcher, M. N. Jones, L. Espada and H. A. Skinner, *J. Chem. Thermodynamics*, 1969, **1**, 381.
[42] L. Espada, M. N. Jones and G. Pilcher, *J. Chem. Thermodynamics*, 1970, **2**, 1.
[43] E. Matijević and B. A. Pethica, *Trans. Faraday Soc.*, 1958, **54**, 587.
[44] P. Mukerjee, *J. Phys. Chem.*, 1972, **76**, 565.
[45] R. J. Cherry, *FEBS Letters*, 1975, **55**, 1.
[46] S. Batzri and E. D. Korn, *Biochim. Biophys. Acta*, 1973, **298**, 1015.
[47] C. Huang and J. P. Charlton, *Biochim. Biophys. Acta*, 1972, **46**, 1660; M. Roseman, B. J. Litman and T. E. Thompson, *Biochemistry*, 1975, **14**, 4826.
[48] L. W. Johnson, M. E. Hughes and D. B. Zilversmit, *Biochim. Biophys. Acta*, 1975, **375**, 176.
[49] J. E. Rothman and E. A. Dawidowicz, *Biochemistry*, 1975, **14**, 2809.
[50] H. Hauser and M. D. Barratt, *Biochim. Biophys. Res. Comm.*, 1973, **53**, 399.
[51] D. M. Small, *J. Lipid Res.*, 1967, **8**, 551.
[52] F. Reiss-Husson, *J. Mol. Biol.*, 1967, **25**, 363.
[53] A. J. Verkleij, B. de Kruyff, P. H. J. Th. Vervegaert, J. F. Tocanne and L. L. M. van Deenen, *Biochim. Biophys. Acta*, 1974, **339**, 432.
[54] T. E. Thompson, C. Huang and B. J. Litman, in *The Cell Surface in Development*, ed. A. A. Moscona (John Wiley, 1974), chap. 1.
[55] D. M. Michaelson, A. F. Horwitz and M. P. Klein, *Biochemistry*, 1973, **12**, 2637.
[56] R. D. Kornberg and H. M. McConnell, *Biochem.*, 1971, **10**, 1111.
[57] M. P. Sheetz and S. I. Chan, *Biochem.*, 1972, **11**, 4573.
[58] J. A. Berden, R. W. Barker and G. K. Radda, *Biochim. Biophys. Acta*, 1975, **375**, 186.
[59] V. F. Bystrov, Y. E. Shapiro, A. V. Viktorov, L. I. Barsukov and L. D. Bergelson, *FEBS Letters*, 1972, **25**, 337.
[60] B. de Kruijff, P. R. Cullis and G. K. Radda, *Biochim. Biophys. Acta*, 1975, **406**, 6.
[61] C. H. Huang, J. P. Snipe, S. T. Chow and R. Bruce-Martin, *Proc. Nat. Acad. Sci. U.S.A.*, 1974, **71**, 359.
[62] S. M. Johnson, *Biochim. Biophys. Acta*, 1973, **307**, 27.
[63] D. Papahadjopoulos and N. Miller, *Biochim. Biophys. Acta*, 1967, **135**, 624.
[64] L. de Bernard, *Bull. Soc. Chim. Biol.*, 1958, **40**, 11.
[65] D. A. Shah and J. H. Schulman, *J. Lipid Res.*, 1967, **8**, 227.
[66] J. Requena, D. A. Haydon and S. B. Hladky, *Biophys. J.*, 1975, **15**, 77.
[67] R. P. Rand, *Biophys. J.*, 1964, **4**, 303.
[68] L. Huang and R. E. Pagano, *J. Cell Biol.*, 1975, **67**, 38.
[69] D. Papahadjopoulos and G. Poste, *Biophys. J.*, 1975, **15**, 945.

[70] R. E. Pagano and L. Huang, *J. Cell Biol.*, 1975, **67**, 49.
[71] R. P. Brand, D. O. Tinker and P. G. Fast, *Chem. Phys. Lipids*, 1971, **6**, 333.
[72] V. Luzzati and F. Husson, *J. Cell Biol.*, 1962, **12**, 207.
[73] V. A. Parsegian, *Trans. Faraday Soc.*, 1966, **62**, 848.
[74] M. Locke and P. Huie, *Science*, 1975, **188**, 1219.
[75] D. W. Fawcett, *An Atlas of Fine Structure: The Cell, Its Organelles and Inclusions* (W. B. Saunders, Philadelphia & London, 1966).
[76] K. R. Porter and M. A. Bonneville, *Fine Structure of Cells and Tissues* (Lea and Febiger, Philadelphia, 4th edn, 1973).
[77] K. M. Yamada, B. S. Spooner and N. K. Wessels, *Proc. Nat. Acad. Sci. U.S.A.*, 1970, **66**, 1206.
[78] R. E. Fine and D. Bray, *Nature N.B.*, 1971, **234**, 115.
[79] M. Daniels, *Ann. New York Acad. Sci.*, 1975, **253**, 535.
[80] K. T. Edds, *J. Cell Biol.*, 1975, **67**, 103a.
[81] B. S. Eckert and R. H. Warren, *J. Cell Biol.*, 1975, **67**, 103a.
[82] see *The Biology of Cytoplasmic Microtubules* (*Ann. New York Acad. Sci.*), 1975, **253**.
[83] J. N. Israelachvili and M. Wilson, *Biological Cybernetics*, 1976, **21**, 9.
[84] J. N. Israelachvili, R. A. Sammut and A. W. Snyder, *Vision Res.*, 1975, **16**, 44.
[85] B. Tandler and C. L. Hoppel, *Mitochondria* (Academic Press, N.Y. and London, 1972), pp. 1-10.
[86] A. L. Lehninger, *The Mitochondrion* (W. A. Benjamin, N.Y. and Amsterdam, 1964), pp. 23-29.
[87] D. Atkinson, H. Hauser, G. G. Shipley and J. M. Stubbs, *Biochim. Biophys. Acta*, 1974, **339**, 10.
[88] D. Papahadjopoulos and S. Ohki, *Science*, 1969, **164**, 1075.
[89] D. Papahadjopoulos, G. Poste, B. E. Schaeffer and W. J. Vail, *Biochim. Biophys. Acta*, 1974, **352**, 10.
[90] D. Papahadjopoulos, W. J. Vail, K. Jacobson and G. Poste, *Biochim. Biophys. Acta*, 1975, **394**, 483.
[91] J. Lansman and D. H. Haynes, *Biochim. Biophys. Acta*, 1975, **394**, 335.
[92] J. N. Israelachvili and D. J. Mitchell, *Biochim. Biophys. Acta*, 1975, **389**, 13.
[93] M. P. Sheetz and S. J. Singer, *Proc. Nat. Acad. Sci. U.S.A.*, 1974, **71**, 4457.
[94] S. Marčelja, *Biochim. Biophys. Acta*, 1974, **367**, 165.
[95] A. Erdélyi, W. Magnus, F. Oberhettinger and F. G. Tricomi, *Tables of Integral Transforms* (McGraw-Hill, New York, 1954), vol. 1.
[96] M. L. Glasser, *J. Math. Phys.*, 1973, **14**, 701.
[97] A. Erdélyi, W. Magnus, F. Oberhettinger and F. G. Tricomi, *Higher Transcendental Functions* (McGraw-Hill, New York, 1954), vol. 1.

(PAPER 5/2173)